Haggerty, J.A., Premoli Silva, I., Rack, F., and McNutt, M.K. (Eds.), 1995
Proceedings of the Ocean Drilling Program, Scientific Results, Vol. 144

33. PHYSIOGRAPHY AND ARCHITECTURE OF MARSHALL ISLANDS GUYOTS DRILLED DURING LEG 144: GEOPHYSICAL CONSTRAINTS ON PLATFORM DEVELOPMENT[1]

Douglas D. Bergersen[2]

ABSTRACT

Drilling during Ocean Drilling Program Leg 144 provided much needed stratigraphic control on guyots in the Marshall Islands. Information from geophysical surveys conducted before drilling and the ages and lithologies assigned to the sediments sampled during Leg 144 make it possible to compare the submerged platforms of Limalok, Lo-En, and Wodejebato with each other and with various islands and atolls in the Hawaiian and French Polynesian chains. The gross physiography and stratigraphy of the platforms drilled during Leg 144 are similar in many respects to modern islands and atolls in French Polynesia: perimeter ridges bound lagoon sediments, transition zones of clay and altered volcaniclastic sediments separate the shallow-water platform carbonates from the underlying volcanic flows, and basement highs rise toward the center of the platforms. Ridges extending from the flanks of these guyots conform in number to rift zones observed on Hawaiian volcanoes. Edifices appear to remain unstable after moving away from the hotspot swell on the basis of fault blocks perched along the flanks of the guyots.

The apparent absence of an extensive carbonate platform on Lo-En, the 100-m-thick sequence of Late Cretaceous shallow-water carbonates on Wodejebato, and the 230-m-thick sequence of Paleocene to middle Eocene platform carbonates on Limalok relate to differing episodes of volcanism, uplift, and subsidence affecting platform development. I analyze three tectonic components to explain these differences in platform development: plate flexure, thermal subsidence of the plate, and edifice size. Flexure modeling on the Anewetak–Lo-En pair suggests that Lo-En lay slightly on the moat side of the flexural arch formed during the construction of Anewetak. The model results are consistent with the negligible difference between the depths to the top of the volcanic substrate of these two guyots and the slight tilting of the Lo-En summit plateau toward Anewetak. The stresses and subsidence associated with flexure of the plate may explain the high-backscatter, cone- and lobe-shaped features cropping out along the flat summit plateau of Lo-En and the absence of an appreciable accumulation of shallow-water carbonate sediments. Age controls on Pikinni-Wodejebato and Mili-Limalok are poor, but flexure modeling on these two pairs of edifices suggests that Pikinni and Wodejebato were probably constructed at approximately the same time, and that construction of a volcano to the south of Limalok may explain a southward fanning of seismic basement reflectors. Neither flexure nor thermal subsidence of the plate appears to be responsible for the demise of the carbonate platforms on top of Wodejebato and Limalok guyots, but uplift or subsidence caused by plate loading may have influenced stratal patterns within the carbonate sediments. Clearly, the use of submerged carbonate platforms drilled during Leg 144 as "dipsticks" for recording the history of Cretaceous sea-level fluctuations requires a better understanding of the sequence and timing of volcanism and mass-wasting in the Marshall Islands. Platform size may have influenced the survival of selected platforms by preventing complete truncation during sea-level lows, but their failure to keep pace with a rise in sea level probably resulted from environmental stresses slowing the rate of productivity.

INTRODUCTION

In recent years, the western portion of the Pacific Plate has become the focus of a number of programs designed to gather information on Cretaceous mid-plate volcanism and sea-level changes. This region is notable for an anomalously shallow seafloor depth in comparison with other ocean basins of similar age, and for a relatively high concentration of seamounts, atolls, guyots, and mid-ocean plateaus. Menard (1964) postulated that the excessive volcanism resulted from fracturing of the plate over a mantle bulge. He called the region the "Darwin Rise." With the advent of plate tectonics and subsequent age estimates for volcanic features within the area extending from the Mid-Pacific Mountains to the Ontong-Java Plateau, this portion of the Pacific Plate was shown to be near the present-day location of French Polynesia at the time of the volcanism (e.g., Smith et al., 1989; Pringle, 1992; Lincoln et al., 1993). Accordingly, the islands composing French Polynesia supply important clues for deciphering the tectonic history of the Marshall Islands (Fig. 1).

French Polynesia consists of five island chains trending in a northwest direction. From northeast to southwest, these chains are the Marquesas Islands, the Gambier-Pitcairn Islands, the Tuamotu Islands, the Society Islands, and the Austral-Cook Islands. Four of these five chains can be directly linked to mid-plate volcanism associated with hotspots; the Tuamotu Islands are the exception, as they appear to be a series of uplifted atolls superimposed on an aseismic ridge (e.g., Duncan and McDougall, 1974, 1976; Turner and Jarrard, 1982). Geophysical and geochemical studies in and around the French Polynesian islands show that this region is similar to the Marshall Islands in such respects as anomalously shallow seafloor and multiple, linear island chains (McNutt and Fischer, 1987). Other characteristics of French Polynesia may also apply to the Marshall Islands, including an apparent overprinting of volcanic events on selected islands and the uplift of neighboring islands through volcanic loading and plate flexure (Duncan and McDougall, 1974, 1976; McNutt and Menard, 1978; Turner and Jarrard, 1982). These observations combined with the distinct geochemical signature of basalt samples (Hart, 1984), the shallow low-velocity zone for Love waves (Nishimura and Forsyth, 1985), and the small estimates for the effective elastic plate thickness (Calmant and Cazenave, 1987) led to the hypothesis that a large mantle plume, or "superswell," perturbs normal plate subsidence in this region (McNutt and Fischer, 1987; McNutt and Judge, 1990). Such a plume may also have been active during the Cretaceous and responsible, therefore, for the apparent similarities in volcanism and subsidence across French Polynesia and the Darwin Rise (e.g., McNutt et al., 1990; Larson, 1992).

The results from Ocean Drilling Program (ODP) Leg 130 (Ontong-Java Plateau), Leg 143 (Mid-Pacific Mountains), and Leg 144 (Marshall Islands, Wake Islands, and Japanese Seamounts) continue to refine the genetic links established between the Darwin Rise and

[1] Haggerty, J.A., Premoli Silva, I., Rack, F., and McNutt, M.K. (Eds.), 1995. *Proc. ODP, Sci. Results,* 144: College Station, TX (Ocean Drilling Program).

[2] Department of Geology and Geophysics, University of Sydney, New South Wales 2006, Australia.

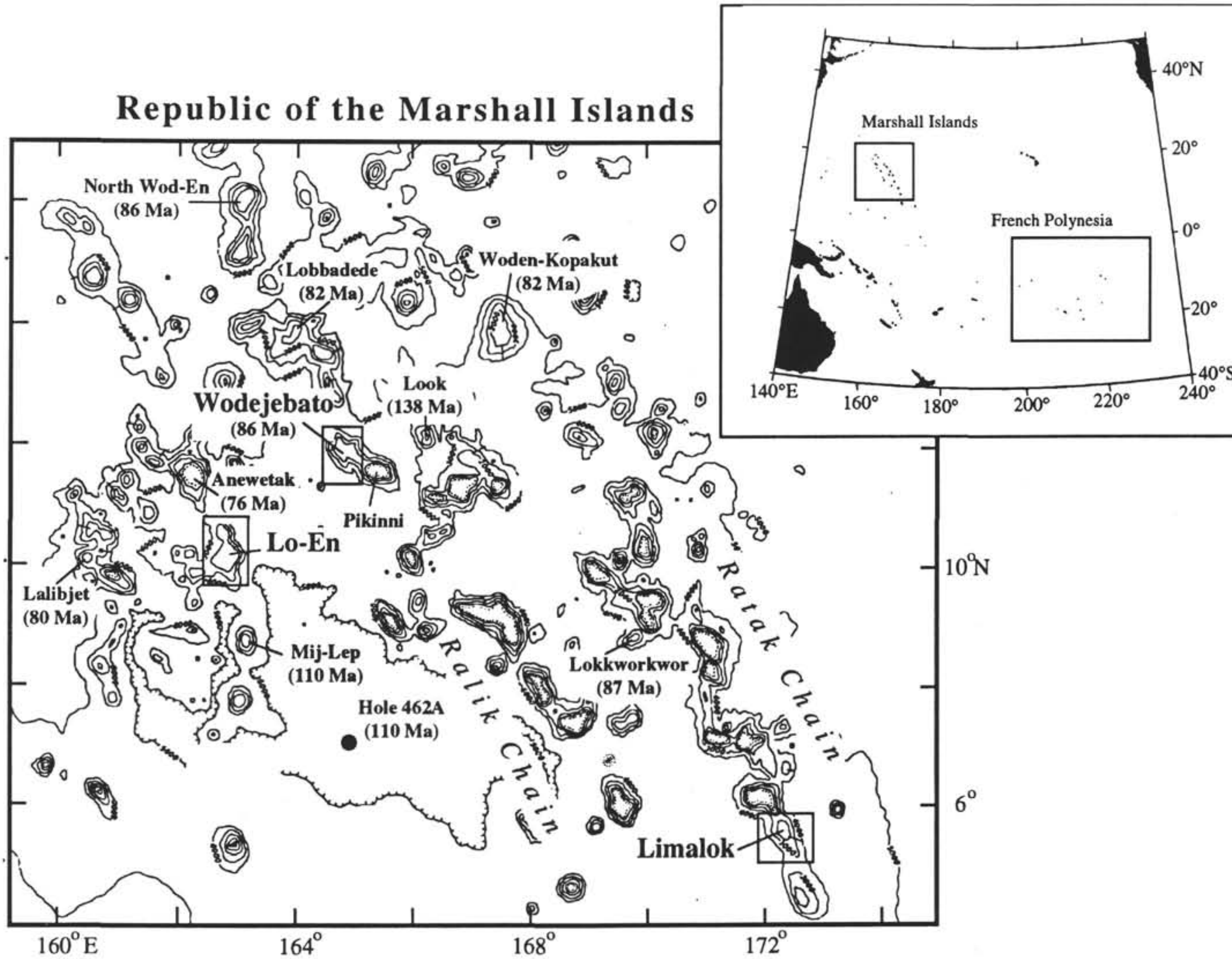

Figure 1. Location map for the Marshall Islands and French Polynesia (inset). Boxes mark the guyots discussed in this paper. The dates shown in parentheses represent radiometric ages of basalts recovered during dredging or drilling; these dates come from Davis et al. (1989), Lincoln et al. (1993), Pringle (1992), and Pringle and Duncan (this volume). Bathymetric map revised from Hein et al. (1990).

French Polynesia. The primary focus of the atoll and guyot drilling legs (143 and 144) was to better understand the Cretaceous history of sea-level changes, platform development, and episodes of volcanism across the Pacific Plate as recorded by the shallow-water carbonate and volcanogenic sediments deposited on top of and adjacent to selected edifices. Inherent in this drilling strategy was the assumption that the thermal subsidence history for these guyots could be modeled and removed from the sediment record to give an indication of eustatic changes in sea level during the Cretaceous. As suggested by the uplifted atolls and islands in French Polynesia (Duncan and McDougall, 1974, 1976; McNutt and Menard, 1978; Turner and Jarrard, 1982), a simple subsidence pattern may not exist in the Marshall Islands. This paper compares the physiography, lithology, and architecture of the platforms drilled during Leg 144 to modern examples in the Hawaiian and French Polynesian chains to (1) identify mechanisms involved in the evolution of the Marshall Islands and (2) determine the importance of plate flexure, relative to thermal subsidence and edifice size, on the development and demise of the carbonate platforms.

BACKGROUND

The Marshall Islands can be subdivided into three geographic provinces: to the east lies the Ratak Chain, to the west lies a cluster of edifices grouped around Anewetak and Ujlan atolls, and between these two groups lies the Ralik Chain. Early models explaining the evolution of volcanic chains within the Marshall Islands were derived from drilling on Anewetak (formerly Enewetak) and Pikinni (formerly Bikini) atolls during Operation Crossroads (Emery et al., 1954; Schlanger, 1963). The atoll drilling provided the first estimates of volcanic platform age and depth in the Marshall Islands and allowed comparisons between two shallow-water carbonate platforms (e.g., stratigraphy, thickness, and age of carbonate sediments; depth to various solution horizons). Two deep holes drilled on Anewetak (Fig. 2) reached the top of the volcanic substrate between 1405 m (Elugelab Island in the northwest) and 1282 m (Parry Island in the southeast; Emery et al., 1954; Schlanger, 1963). Drilling on Pikinni Atoll consisted of four holes (Fig. 2), the deepest of which penetrated 779 m of shallow-water sediments but did not encounter basalt basement (Cole, 1954; Emery et al., 1954). The average depth to the top of the volcanic substrate on Pikinni was estimated by Raitt (1954) from seismic refraction data to lie around 1300 m, although he noted the data support a depth range between 600 and 2100 m. On Anewetak Atoll, Eocene shallow-water carbonate sediments lay directly over the basalt, originally dated by K/Ar methods as 51.4 to 61.4 Ma, but later dated by $^{40}Ar/^{39}Ar$ methods to produce an age of 75.9 ± 0.6 m.y. (Pringle, 1992). As the volcanic platform beneath Pikinni was not sampled, its age has not been measured.

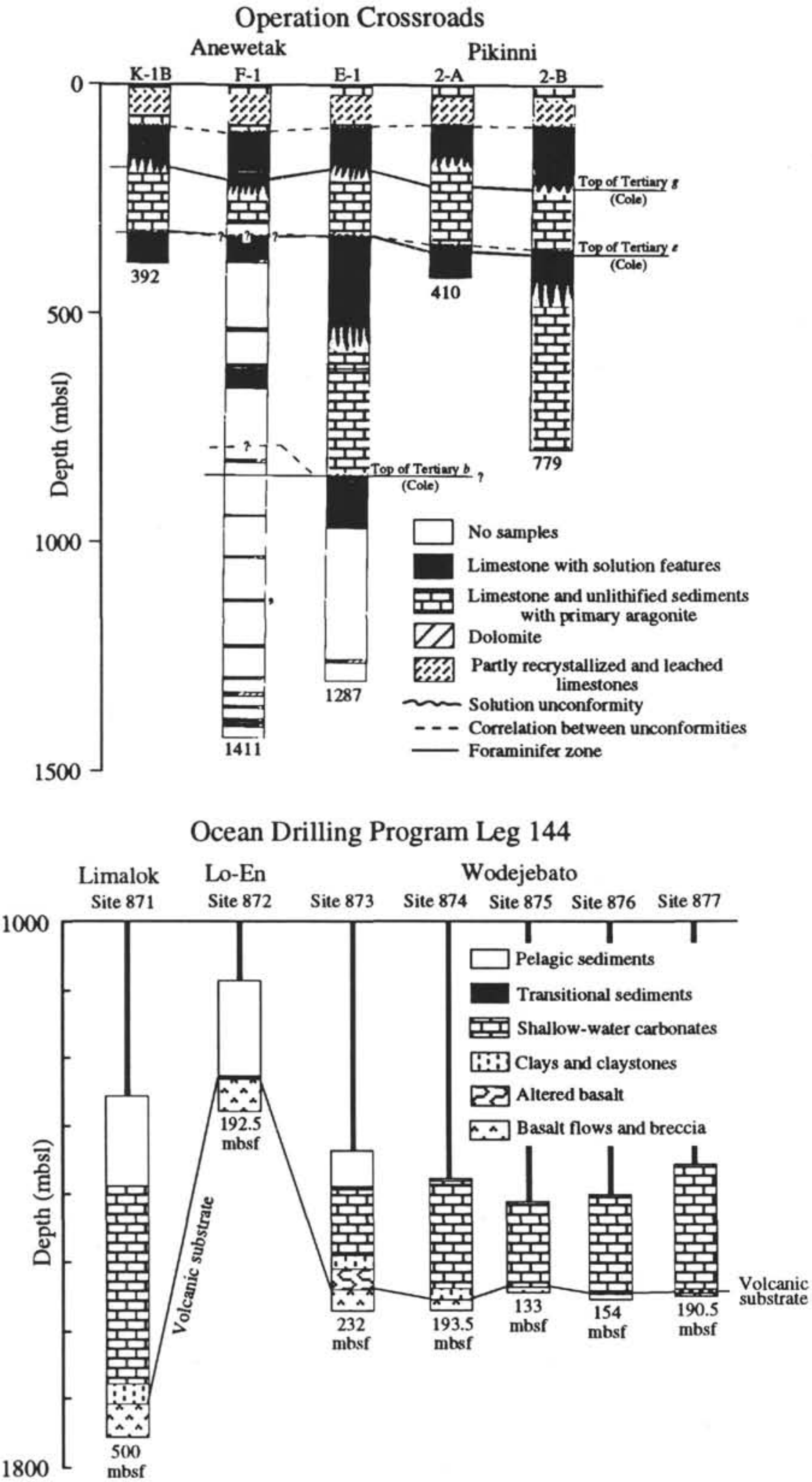

Figure 2. Stratigraphy of cores drilled on Anewetak and Pikinni atolls during Operation Crossroads and on Limalok, Lo-En, and Wodejebato guyots during Leg 144. Site locations shown in subsequent figures.

The model developed by Schlanger (1963) for the Marshall Islands, on the basis of the atoll drilling, was that shallow-water carbonate platforms of Eocene age grew on top of Cenozoic-age volcanic platforms. These platforms subsided at anomalously fast rates, given the age of the plate upon which they were built (Detrick and Crough, 1978). The shallow-water carbonate sediments recorded a series of relative sea-level falls in the form of solution unconformities, and the good correlation between the depths of these unconformities across the two carbonate platforms suggested that these sea-level changes were eustatic in nature. Accordingly, atolls and guyots became viewed as mid-ocean "dipsticks" upon which eustatic changes in sea level were recorded.

Questions concerning the history of volcanism in the Marshall Islands, and the Cretaceous in general, began to arise with the drilling results from Deep Sea Drilling Program (DSDP) Legs 61 and 89. Both legs spent time drilling or deepening a hole west of the Marshall Islands in the Nauru Basin. Hole 462 penetrated a total of 599 m of sediment and 18 m of basalt; Hole 462A extended "basement" penetration an additional 451 m into the basalt complex (Larson, Schlanger, et al., 1981; Moberly, Schlanger, et al., 1986). The lowermost unit at this site consists of basalt sheet flows overlain by single and multiple basalt sills, all of which are normally magnetized (presumably erupted during the Cretaceous normal superchron). Microfossils in the sediment layer separating the flow complex from the overlying sill units suggest that the youngest flows are ~112 m.y. (Moberly, Schlanger, et al., 1986), whereas radiometric dating of the oldest flows shows an age range between 127 and 131 m.y. (Takigami et al., 1986). Farther up in the hole, redeposited shallow-water sands, reef limestones, phosphorite, and subaerial basalt indicate nearby edifice-building during the Campanian and Maastrichtian (~75–80 Ma; e.g., Premoli Silva and Sliter, 1981). The results from Site 462 provided a better perspective, in comparison with those afforded by the Operation Crossroads drilling, on the extent and types of volcanic events affecting this portion of the Pacific Plate during the Cretaceous. From the drilling data, Schlanger and Premoli Silva (1981) postulated that plate uplift and major mid-plate volcanism began in Barremian to early Aptian time (~115 Ma) and continued intermittently through the Maastrichtian. Alternatively, Moberly and Jenkyns (1981) proposed two distinct episodes of mid-plate volcanism, one at 118 ± 6 Ma and another at 74 ± 2 Ma. Both models extended the beginning of edifice building in the Marshall Islands back to the mid-Cretaceous, consistent with results from Site 462.

Dredging across the guyots composing the Marshall Islands during the 1988 *Moana Wave* Cruise MW8805 provided the next information concerning their evolution. Samples collected during this cruise varied widely in composition (e.g., basalt, basalt conglomerates, shallow-water carbonates) and age (mid-Cretaceous to middle Eocene), and were the basis for a more refined model detailing the Cretaceous history of volcanism and carbonate platform growth in this region. Lincoln et al. (1993) used the age information from the fossil constituents of shallow-water carbonates and carbonate cements and the radiometric dating of basalts to develop a multiple hotspot model for the evolution of the Marshall Islands. They proposed that, as the portion of the Pacific Plate containing the Marshall Islands moved away from the East Pacific Rise during the Cretaceous, it was influenced by the swells from at least two aligned hotspots, similar to the present situation in French Polynesia (e.g., the Mehetia and Rurutu hotspots; Turner and Jarrard, 1982). Uplift and volcanism associated with these hotspot swells resulted in two sequences of reef growth across many of the edifices in the Marshall Islands.

The fossil content of limestones recovered in rock dredge (RD) 50 from Wodejebato Guyot during Cruise MW8805 was central to the development of this model. These limestones contain rudists, interpreted as Albian in age (~100 Ma), in a matrix of shallow-water foraminifers (Campanian to Maastrichtian in age, ~75–80 Ma). Radiometric dating of a basalt sample collected along the north flank of Wodejebato during the Mid-Pacific Expedition (MP43-D; Hamilton and Rex, 1959) placed the latest stage of volcanism at ~86 Ma (M. Pringle, pers. comm., 1991). Thus, the interpretation that the edifice was at sea level during the Albian and Late Cretaceous, on the basis of the limestone fossil assemblage, was only substantiated for a Late Cretaceous volcanic episode (and presumably edifice uplift) on the basis of the radiometric age. Other edifices from which mid-Cretaceous carbonate sediments were dredged during Cruise MW8805 include Lo-En, Lewa, Lobbadede, and Ruwituntun guyots, with ages ranging from latest Albian to earliest Cenomanian (Fig. 1; Lincoln et al., 1993). Lo-En Guyot is of interest here because of its proximity to Anewetak Atoll. Planktonic foraminifers and calpionellids within the matrix of a breccia recovered in RD33 along the southwest flank of Lo-En (~2400 m depth) are interpreted as evidence of a near-shore environment during the early to middle Albian time (Lincoln et al., 1993). Two other dredges on this guyot (RD34 and RD35) sampled shallower portions of the slope (~1900 and ~1775 m, respectively) and recovered rounded basalt cobbles and basalt pebbles in matrixes containing planktonic foraminifers of Paleogene age. Although no direct evidence in the MW8805 data supported an episode of Late Cretaceous volcanism or reef growth on Lo-En, Lincoln et al. (1993) postulated that uplift and subaerial exposure of this edifice was likely around the time of volcanic activity on Anewetak Atoll (~76 Ma). Radiometric ages for basalts dredged from guyots throughout the Marshall Islands appear to contradict this "mid-Cretaceous/Late Cretaceous" model for plate uplift and volcanism. Pringle and Staudigel (1992) show that the majority of basalts dated from this region fall between 90 and 75 m.y. Only two guyots, Look and Mij-Lep, exhibit ages older than 100 Ma (Fig. 1), and neither of these edifices is capped by a carbonate platform. Consequently, very few radiometric ages support extensive edifice building in the Marshall Islands during the mid-Cretaceous.

The early Tertiary development of carbonate platforms in the Marshall Islands is best represented by Limalok Guyot. Dredges across Limalok during a 1981 *Kana Keoki* cruise (KK810626, Leg 2) returned a mixture of shallow-water carbonates within a planktonic foraminifer matrix, indicating a complex history of platform growth and subsequent redeposition in a deeper water environment (Schlanger et al., 1987). Large benthic foraminifers within the limestones suggest that the carbonate platform was established by the early Eocene. Schlanger et al. (1987) postulated that Eocene sea-level changes, apparently derived from the eustacy curves of Vail et al. (1977), resulted in emergence and later resubmergence of the carbonate platform. Lincoln (1990) attempted to constrain the history of emergence and subsidence across this carbonate platform by examining the carbon and oxygen isotope compositions of the limestones in Dredges KK81-4 and KK81-6. Analyses on both the primary fossil components (foraminifers and red algae) and the cements failed to support the existence of a subaerial exposure event affecting the limestones capping Limalok, nor did they provide any additional information on when or why this carbonate platform failed.

In summary, the models for edifice construction and shallow-water platform growth in the Marshall Islands before Leg 144 drilling consisted of two episodes of Cretaceous volcanism, uplift, and subsidence separated by as much as 30 m.y. for Lo-En and Wodejebato guyots, and a single episode of Eocene edifice construction and subsidence for Limalok Guyot. A principle factor affecting platform development is the ability of reefal organisms to colonize the subsiding volcanic pedestal. Carbonate platform growth requires that a balance be established between the net vertical accretion rate of the organisms responsible for producing the carbonate sediment and the relative rate of sea-level rise. Net vertical accretion rates for modern reef systems range from approximately 1 to 10 mm/yr, although these rates vary with water depth, temperature, nutrient content, and turbidity (e.g., Schlager, 1981; Buddemeir and Smith, 1988; Grigg and Epp, 1989). Rates of relative sea-level rise, on the other hand, include the effects of plate subsidence away from a spreading ridge or hotspot, plate flexure caused by volcanic or sediment loading, and eustatic changes in sea level. To date, plate flexure has not been included in the models for platform development in the Marshall Islands. The purpose of this paper is to relate the observed platform stratigraphy and architecture to the combined effects of plate flexure and those presumably produced by thermal subsidence and consequent edifice truncation.

METHODOLOGY

The new data presented in this paper consist primarily of SeaMARC II sidescan sonar images and swath bathymetry, SeaBeam multibeam bathymetry, analog and digital single-channel seismic profiles, six-channel seismic profiles, and 3.5-kHz echo sounder profiles. Observations from these data, together with published studies of French Polynesia, are used to model the flexure caused by volcanic loading around the edifices of Limalok, Lo-En, and Wodejebato guyots. The effects of plate flexure on these three guyots are presented in a later section of this paper. This section describes the acquisition and processing schemes applied to the data, and the model used to estimate plate flexure in the Marshall Islands.

Sidescan Sonar Images

Detailed surface mapping of Limalok, Lo-En, and Wodejebato guyots was accomplished with the shallow-towed, sidescan sonar system SeaMARC II. This system, before its loss at sea in 1991, was capable of collecting acoustic backscatter data in swaths up to 10 km wide and bathymetric data with a swath width equal to 3.4 times the water depth. The system operated at frequencies of 11 kHz on the port side and 12 kHz on the starboard side. Blackinton (1986) and Shor (1990) provide a thorough description of the system and its capabilities.

Sidescan resolution is a function of many variables and is both range and orientation dependent. The resolution of the SeaMARC II system is on the order of several tens of meters in normal ocean depths (Johnson and Helferty, 1990). Corrections applied to the backscatter data compensate for errors in slant range (based on water depth below the tow vehicle), beam pattern, bottom tracking, and gain variations. The data, in the form of ~10^3 pixels on each side per ping, are displayed as gray-scale images. Individual 10-km-wide image swaths for the various tracks are assembled into a mosaic of the survey area. In this paper, dark gray to black tones represent areas of higher backscatter and shades of light gray to white represent areas of lower backscatter and acoustic shadows. Cruise KK820402 was one of the first test cruises for the SeaMARC II system; during this leg, only the starboard-side transducer arrays were connected (see sidescan images over Limalok). During Cruise MW8805, the starboard arrays malfunctioned; although it was still possible to collect backscatter data from both sides of the tow vehicle, the starboard-side data are clipped at both the high and low ends of the recording spectrum. This clipping resulted in images with few data values in the mid-range gray tones (see sidescan images over Lo-En and Wodejebato).

Further distortion of the images occurs by the application of a "flat-bottom" assumption (i.e., the seafloor is flat beneath the tow vehicle) before data recording. The result is a small error in geographic positioning of features where the bottom topography slopes in relation to the tow-vehicle track (e.g., when surveying parallel to the slope of the guyot, features on the up-dip side of the tow vehicle are positioned anomalously far from the ship track, and vice versa).

Digital Seismic Data

A single-channel streamer was used to collect digital seismic data during Cruise MW8805. When the SeaMARC II tow vehicle was in the water, the source was a 120-in.^{3} air gun; at other times, an 80-in.^{3} water gun was used. Processing of the data included band-pass filtering from 10 to 100 Hz, automatic gain control, deconvolution, and muting of water noise. During Cruise MW9009, a six-channel streamer was used with a pair of synchronized 80-in.^{3} water guns. In addition to the processing routines applied to the single-channel data, the six-channel data were gathered, stacked, and migrated.

Flexure Model and Model Parameters

A number of geophysics and geodynamics texts review in detail the concepts important to evaluating plate elasticity and flexure (e.g., Menke and Abbott, 1990). The following discussion is only a brief overview of this information.

The most critical, and in the case of the Marshall Islands the least known, piece of information necessary for building a well-constrained flexure model is the time of plate loading in relation to other features on the plate. The scattered distribution of radiometric and fossil ages illustrates that such information on a regional scale is sorely lacking in this area (Fig. 1). Leg 144 drilling provides good age control on the volcanic and carbonate platforms composing Lo-En, Wodejebato, and Limalok, especially in relation to previous drilling results on Anewetak and Pikinni atolls. For example, $^{40}Ar/^{39}Ar$ dating of the basalts recovered during Leg 144 shows that the best age for the volcanic platform of Lo-En (112.8 ± 1.2 m.y.; Pringle and Duncan, this volume) is much older than that of Anewetak (75.9 ± 0.6 Ma; Pringle, 1992). By making some assumptions on the age of the edifice beneath Pikinni, the implications of flexure on these two atoll and guyot pairs can be examined. In turn, application of the results on Pikinni and Wodejebato allow flexure modeling for the edifices around Limalok.

In addition to the timing of loading, the following plate and load parameters must be specified to build a flexure model: (1) type of plate behavior in response to a surface load (i.e., elastic or viscoelastic); (2) effective elastic thickness of the plate and the viscous relaxation time; (3) dimensions of the load (e.g., height, basal radius, slope); and (4) mantle, load, infill sediment, and water densities.

Calment and Cazenave (1986) show that little evidence exists in the geoid data over the Cook-Austral and Society chains to suggest that a viscoelastic model is appropriate for the plate beneath these islands (i.e., plate thickness apparently decreasing with increasing age). As previous studies show that selected Marshall Islands edifices rotate back through time to the area of the Cook-Austral and Society chains (e.g., Smith et al., 1989; Lincoln et al., 1993; Bergersen, this volume), I use an elastic plate model in all flexure calculations.

Assuming that (1) Earth's lithosphere acts as an elastic shell overlying a fluid medium, (2) the flexural rigidity of the plate is constant, and (3) no horizontal or tensile stresses are present within the plate before the flexural deformation, then the differential equation for three-dimensional plate flexure simplifies to

$$D\,\nabla^4 w + (\rho_m - \rho_i)\, g w = q\,, \qquad (1)$$

where D is the flexural rigidity of the plate $\{D = E\,T_e^{\,3} / [12(1-\upsilon^2)]\}$; w is the vertical displacement in response to a load; ρ_m and ρ_i are the densities of the mantle and infill, respectively; g is the gravitational constant (9.8 m/s^2); and q is the load $[(\rho_l - \rho_w)gh]$. The term $(\rho_m - \rho_i)gw$ accounts for the buoyancy force acting beneath the load as material filling the moat displaces mantle material within the region of deflection. In the definition for the flexural rigidity of the plate (D), T_e represents the elastic thickness of the plate, E is Young's modulus, and υ is Poisson's ratio. The h in the definition for the load (q) represents the height of the load, and ρ_l and ρ_w are the density of the load material and water, respectively.

Three-dimensional plate flexure can also be determined by finding the response function of a constant rigidity plate to a point load (the Green's function of the system). Because a unit point load on a homogenous plate produces an axisymmetrical deflection, the response (Green's) function can be written in polar coordinates, which allows the derivation of the Green's function in spatial terms:

$$w(r) = q_0\, \gamma^2\, \mathrm{Kei}(\gamma r) / [\, 2\pi\, (\rho_m - \rho_i)\, g\,]\,, \qquad (2)$$

where γ = three-dimensional flexure wave number = $[(\rho_m - \rho_i)\, g\, /\, D]^{1/4}$, and Kei (γr) = the zero-order Kelvin-Bessel function describing axisymmetric deflections about a point load.

Numerical evaluation of the deflection for any load is possible by approximating the load as a number of point loads and by summing the deflections from all these point loads as observed at various points across an area (i.e., convolving the load with the Green's function).

The remaining plate and load parameters used in this paper are approximated from previous flexure modeling in French Polynesia. Models of SEASAT satellite-derived geoid height data over the southeast Pacific provide estimates of the effective elastic plate thickness, which appears to vary between ~8 km beneath the Society, Marquesas, and Pitcairn seamounts and ~13 km beneath the Cook-Austral

Chain (Calmant and Cazenave, 1986, 1987). More recent studies using ship-based gravity measurements suggest elastic plate thickness may be on the order of 23 ± 2 km around the Society Islands and 18 ± 2 km around the Marquesas Islands (Filmer et al., 1993). The only estimate of plate thickness in the Marshall Islands comes from gravity measurements over Woden-Kopakut Guyot (formerly Ratak), which suggest that the volcano was constructed on a plate <15 km thick (Smith, 1990). Lambeck (1981) modeled flexure in the Society Islands using a number of different flexure indicators (e.g., arch distance and amplitude, geoid measurements, regional bathymetry) and different load and fill geometries. He arrived at preferred estimates for the density of the load around 2500 kg/m^3 and the flexural rigidity of the plate ~3×10^{29} N m. These values are very similar to those derived by McNutt and Menard (1978): 2800 kg/m^3 and 2×10^{29} N m. Given that the existing data are insufficient to derive independent estimates of elastic plate thickness for the Marshall Islands, plate thickness in the models presented here varies from 10 to 20 km. The models also use a density of 3300 kg/m^3 for the mantle, 2700 kg/m^3 for the load, 2500 kg/m^3 for the infill, and 1000 kg/m^3 for water. More extreme values for the load and infill densities (maximum values of 3000 and 2500 kg/m^3, and minimum values of 2500 and 2300 kg/m^3, respectively) cause a change in flexure wavelength of <10%.

Modeling the original size and shape of ancient volcanic loads also requires a number of assumptions. The atolls of Anewetak and Pikinni presumably grew on top of the eroded summits of shield volcanoes. Consequently, simple axisymmetrical cones of a given height and basal diameter can be used to represent the volcanic platforms (Fig. 3). The height of each load can be estimated by summing the depth of the undeformed plate at the time of loading with the height of the volcano above sea level. Seismic data between Anewetak and Pikinni, well away from the flexural deformation caused by these loads, show three distinct reflectors beneath the 5120-m-deep seafloor (Fig. 3). The lowermost reflector is assumed to define the undeformed plate depth, which appears around 7.6 s two-way traveltime (TWT). A similar sequence of reflectors lie in the vicinity of Site 462 in the Nauru Basin (Larson, Schlanger, et al., 1981); hence, velocities of 1700 and 2300 m/s were assumed for the two major units overlying the deep reflector. Thus, the total sediment thickness is ~775 m, which produces an undeformed plate depth of 5895 m. This depth estimate does not account for the isostatic effects of sediment loading. Using a 600 m/s correction value to compensate for sediment loading (Crough, 1983b) and subtracting the amount of subsidence brought about by thermal cooling of the plate (~1300 m for Anewetak as shown by the depth to top of the volcanic platform), the corrected plate depth appears to be ~4125 m at the time of loading. This depth is consistent with the 4000 to 4300 m seafloor depths around present-day French Polynesia (e.g., Cheminee et al., 1989; Stoffers et al., 1989). As the volcanic platforms were presumably shield volcanoes and not flat-topped edifices at the time of loading, some mass must be added to the tops of the observed platforms to account for subaerial erosion. The island in French Polynesia that appears most comparable in size to Anewetak and Pikinni is Tahiti-Nui (Table 1), the larger of the two cones forming the island of Tahiti in the Society Chain (Duncan and McDougall, 1974). Tahiti-Nui rises 2241 m above sea level; hence, an additional 2300 m is added to the height of the model loads, resulting in a grand total of 6425 m.

The basal diameter of the volcanoes, buried beneath ~775 m of sediment, cannot be measured directly from bathymetric maps. For the modeling presented in this paper, the basal diameter was estimated by measuring the slope of the flank between two widely spaced contours encircling the edifice (e.g., 1000- and 2000-m contours) and then applying this slope to the portion of the edifice buried beneath the sediments. This method resulted in basal diameters of 100 km for Anewetak Atoll and 90 km for Pikinni Atoll. The shape and size of the loads representing Lo-En and Wodejebato guyots are not important as the modeling conducted in this paper only examines the effects of loading by Anewetak and Pikinni.

Before presenting the results from the flexure modeling, I describe the gross physiography and architecture of the submerged platforms drilled during Leg 144 because these observations will be used, in part, to test the model results. As I show later, the flexure models help explain some of the anomalous features observed on Limalok, Lo-En, and Wodejebato.

GUYOT DESCRIPTIONS AND COMPARISONS TO MODERN ANALOGS

Descriptions of the geological and geophysical data serve to put the drilling results in perspective with the overall structure of the guyot. Ideally, features noted on the Marshall Islands guyots should be similar to features observed on subaerial volcanic islands that have been studied in greater detail. Obvious candidates for such a comparative study include the islands composing Hawaii and French Polynesia (e.g., the Society and Austral chains). When comparing the Marshall Islands to the Hawaiian Islands, one of the problems encountered is a difference in scale: the islands in Hawaii are typically at least twice as large as the edifices drilled in the Marshall Islands. On the other hand, although islands within the Society and Austral chains are more comparable in size to guyots in the Marshall Islands, geological information from French Polynesia is less available. Accordingly, I use examples from both regions to understand similar features noted in the Marshall Islands better.

Limalok Guyot, located between 5°30′ and 5°45′N, and 172°10′ and 172°30′E, lies in the southernmost portion of the Ratak Chain (Fig. 1). Nakanishi et al. (1992b) identified Anomaly M22 near this portion of the Marshalls. Using the time scale of Harland et al. (1990), the crust beneath Limalok is ~155 m.y. The summit plateau narrows slightly from 27 km in the north to 15 km in the south and is ~36 km long (Fig. 4; Table 1). Schlanger et al. (1987) estimated a minimum depth of ~1700 m for the seismic basement reflector, which deepens to ~1900 m toward the margin of the summit plateau. In the sidescan sonar images (Figs. 5, 6), a high-backscatter (dark) band along the perimeter of the summit plateau marks areas where the carbonate complex crops out from the overlying pelagic sediments. Broad terraces, 1 to 4 km wide and up to 12 km long, lie outside the scalloped plateau margin (Table 2). These terraces are most prominent along the south and west sides of the plateau. A volcanic ridge extends ~67 km to the northwest, attaching Limalok to Mili and Knox atolls.

Lo-En Guyot, centered about 10°10′N and 163°52′E, lies ~165 km south-southeast of Anewetak Atoll in the cluster of volcanoes marking the western boundary of the Marshall Islands (Fig. 1). Extrapolation of magnetic lineations identified to the south of these two edifices (Nakanishi et al., 1992b) produces an estimated plate age of >160 m.y. using the time scale of Harland et al. (1990). The summit plateau of Lo-En varies between 30 and 40 km in diameter, with the 1400-m contour generally defining the first major slope break (Fig. 7; Table 1). In the sidescan sonar images, high-backscatter, cone- and lobe-shaped features disrupt the low-backscatter pelagic sediments covering the summit plateau (Figs. 8, 9). One of the high-backscatter, cone-shaped features crossed on the plateau has a summit depression filled with pelagic sediment (Fig. 10) and a relatively large-amplitude magnetic signature. Dredging on this cone during Cruise MW8805 recovered manganese-encrusted basalt breccia containing altered clasts of basalt with oxidized phenocrysts of olivine. Consequently, at least some of these high-backscatter cones are volcanic in composition. Terraces can be seen in the sidescan images along the southwest edge of the edifice, although they are not nearly as large or as distinct as those observed on Limalok (Figs. 8, 9; Table 2). Two volcanic ridges extend from the flanks of Lo-En: one ridge connects this submerged platform to Anewetak Atoll to the north-northwest, whereas a second smaller ridge extends to the south-southeast.

Wodejebato Guyot, located at 12°00′N and 164°50′E, lies in the northernmost portion of the central Ralik Chain, ~60 km northwest of Pikinni Atoll (Fig. 1). As in the case of Lo-En, the >160-m.y. plate age

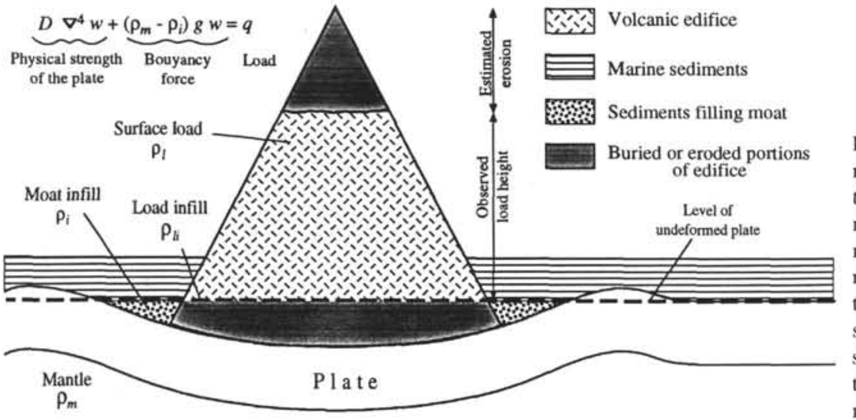

Figure 3. Modeling plate flexure from volcanic loads requires a good understanding of the load dimensions. In the case of the Marshall Islands, a number of assumptions must be made about the load because of erosion and sediment deposition subsequent to the time of load emplacement. Estimated parameters include the original height of the volcano (the observed height plus the amount buried by sediment and the amount removed during subaerial exposure), the density of the edifice (ρ_l and ρ_{li}), the density of the sediment filling the moat (ρ_i), and the density of the mantle (ρ_m).

Table 1. Comparisons between selected Pacific island chains.

	Area (km^2)	Summit plateau length (km)	Width (km)	Episodes of volcanism (m.y.)	Comments
Marshall Islands:					
Limalok	636	36	24	>Paleocene (f)[a]	Carbonate platform submerged by late Eocene. Seismic basement reflectors prograde to the south.
Lo-En	823	42	28	pre-Turonian (f)[a] 112.8 ± 1.2 (r)[b]	No carbonate platform or thick clay weathering horizon encountered at Site 872. Cone- and lobe-shaped features crop out from pelagic sediments.
Wodejebato	505	38	11 to 20	Cenomanian (f)[a] 83.2 ± 1.1 (r)[b]	Shallow-water carbonate platform submerged by middle Maastrichtian (~70 Ma). Cenomanian nannofossils recovered in clay horizon at Site 873.
French Polynesia:					
Cook Islands:					
Raratonga		11.0	7.3	1.6–2.3[c]	Geomorphically young island with very little reef development along its shores. Located southeast of numerous makatea islands.
Aitutaki	14	7.8	2.8	7.39 to >8.73[c] 0.7–1.9[c]	Very nearly an atoll, with carbonate platform area approaching 95 km2. Appears to have two episodes of volcanism separated by ~6 m.y.
Austral Islands:					
Rimatara				>4.78 ± 0.42[c] 20.6–29.9[c]	Uplifted island with 83-m-high volcanic summit and 11-m-high makatea.
Rurutu	35	11.0	5.2	1.06–1.12[c] 12.08–12.56[c,d]	Uplifted remnant of single shield volcano with limestone cliffs up to 100 m high surrounding much of the island. Clay transition zone up to 3 m thick.
Society Islands:					
Tahiti-Nui	1014	37.9	36.2	0.4–1.2[d]	Larger of the two cones forming the island of Tahiti. Reaches a maximum elevation of 2241 m. Similar in size to edifices within the Marshall Islands
Tahiti-Iti	309	26.6	17.5	<0.5[d]	Smaller of the two cones forming Tahiti. Also referred to as Taiarapu. Constructed after Tahiti-Nui.
Moorea	128	14.6	14.2	1.49–1.64[d]	Lies ~16 km northwest of Tahiti. Approximately one third of the cone appears to have eroded.
Huahine	50	10.7	5.7	2.01–2.58[d]	Consists of twin islets encircled by a common barrier reef. Islets represent the remnants of a single cone split by faulting.
Gambier Islands:					
Mururoa	154	27.5	11.1	7.0 ± 1.0[e]	Atoll on which volcanic basement shallows by over 200 m toward the center of cone, and a clay transition zone reaches thicknesses of up to 90 m.
Hawaiian Islands:					
East Maui	1887	77	67	0.75 ± 0.04[f]	Perhaps the most similar island in the Hawaiian Chain to the atoll and guyot pairs in the Marshall Islands.
Mauna Kea	2382	82	40	0.375 ± 0.05[f]	One of the shield volcanoes composing the island of Hawaii. Note the size difference between this volcano and those platforms sampled in the Marshall Islands.

Notes: (f) = fossil age and (r) = $^{40}Ar/^{39}Ar$ radiometric age; other ages determined by K/Ar techniques. References as follows: a = Premoli Silva, Haggerty, Rack, et al. (1993), b = Pringle and Duncan (this volume), c = Turner and Jarrard (1982), d = Duncan and McDougall (1976), e = Duncan et al. (1974), and f = Clague and Dalrymple (1989).

beneath Wodejebato is derived through extrapolation of magnetic anomalies identified in the southern Marshall Islands (Harland et al., 1990; Nakanishi et al., 1992b). The summit plateau of Wodejebato is about 43 km long and increases in width from <12 km in the southeast to >25 km in the northwest (Fig. 11; Table 1). A transition from a steep upper slope (~20°–24°) to a more gently inclined lower slope (~7°) occurs around 2500 m. The 1400 m contour generally marks the first break in slope down from the summit plateau. As in the case of Limalok, the seismic basement reflector shoals toward the center of the summit plateau (Bergersen, 1993). Sidescan sonar images over the summit plateau (Figs. 12, 13) show a high-backscatter band inset slightly from the upper slope of the guyot. Again, similar to Limalok, this high-backscatter band represents areas where the carbonate platform crops out from the overlying pelagic sediments. A well-defined, elongate terrace lies along the south flank of Wodejebato. Four flank ridges extend from the main body of the edifice and, along with the volcanic spur attaching Wodejebato to Pikinni, give the guyot a distinct "starfish" shape.

Physical differences between these three guyots relate directly to differing episodes of volcanism, uplift, subsidence, and erosion. For example, the shallow-water carbonates across the summit plateaus of Limalok and Wodejebato suggest a much different history than the cone- and lobe-shaped features cropping out from the pelagic sediments on Lo-En. The degree to which the history of volcanism, uplift,

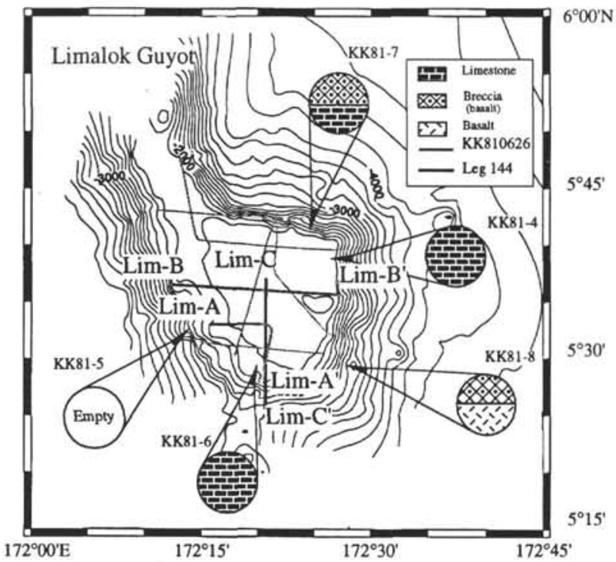

Figure 4. Bathymetric control over Limalok Guyot (formerly Harrie Guyot) is currently limited to echo sounder profiles. Shallow-water carbonates recovered from this guyot are primarily Eocene in age, and the small triangles and accompanying circles show the location and lithology of these dredge samples. Gray lines mark the location of seismic profiles collected during Cruise KK810626 (Leg 2) and Leg 144, with the thicker, annotated lines showing profiles presented in this paper. The contour interval is 200 m. Gridding and contouring of echo-sounder data was accomplished with software developed by Wessel and Smith (1991).

Figure 5. Sidescan sonar images over Limalok Guyot, collected during Cruise KK820402, show a scalloped high-backscatter (dark tones) band inset from the edge of the summit plateau. The band marks the edge of the carbonate platform capping this edifice, and the scalloped configuration of the band results from block-faulting of the platform (see Fig. 6 for geologic interpretation).

Table 2. Flank ridge and fault block dimensions.

	Flank ridge dimensions			Fault block dimensions		
	Area (km^2)	Length (km)	Width (km)	Smallest block (km)	Largest block (km)	Average area (km^2)
Limalok	—	—	—	9.3	12.7	24
Lo-En:				3.5	6.5	5
South FR	181	14.5	14.6			
Wodejebato:				<1	18.2	7
South FR	73	11.3	7.4	—	—	—
West FR	~23	10.8	~1.8	—	—	—
North FR	54	12.2	7.0	—	—	—
Northeast FR	12	~1.6	6.4	—	—	—
	(Portion attached to shelf)					
	~29	~6.6	~5.9	—	—	—
	(Isolated hill adjacent to edifice)					

Notes: FR = flank ridge. Dashes (—) = null values.

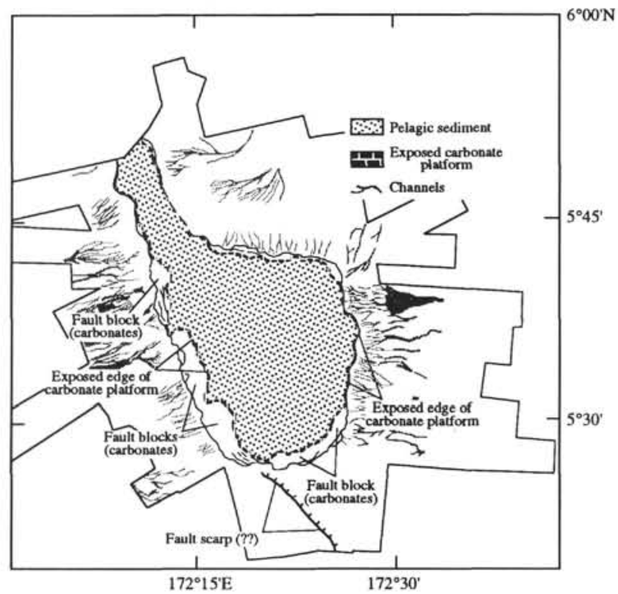

Figure 6. Geologic interpretation of sidescan images over Limalok Guyot showing the major geomorphic features as related to their backscatter characteristics.

and subsidence differs across these three edifices can be defined by comparing the following features found in common: ridges extending from the flanks of the edifice, terraces located downslope from the first slope break, and the composition and architecture of sediment units across the relatively flat summit plateaus.

Flank Ridges

I use the term "flank ridge" in this paper to avoid any confusion between the assumed and known origin for these features. Rift zones, as observed in the Hawaiian Islands, are zones of volcanic features associated with underlying dike complexes (Bates and Jackson, 1980). Vogt and Smoot (1984) introduced the concept that ridges extending from the flanks of seamounts and guyots (their "flank rift zones") are analogous to rift zones observed on volcanic islands. The evidence they cite supporting this relationship is the physiography of the ridges as observed in multibeam bathymetric maps. Seamounts located off the flanks of a guyot or the erosional remnants left behind after large-scale landslides may also appear in bathymetric maps as relatively continuous ridges, thus complicating the apparently simple

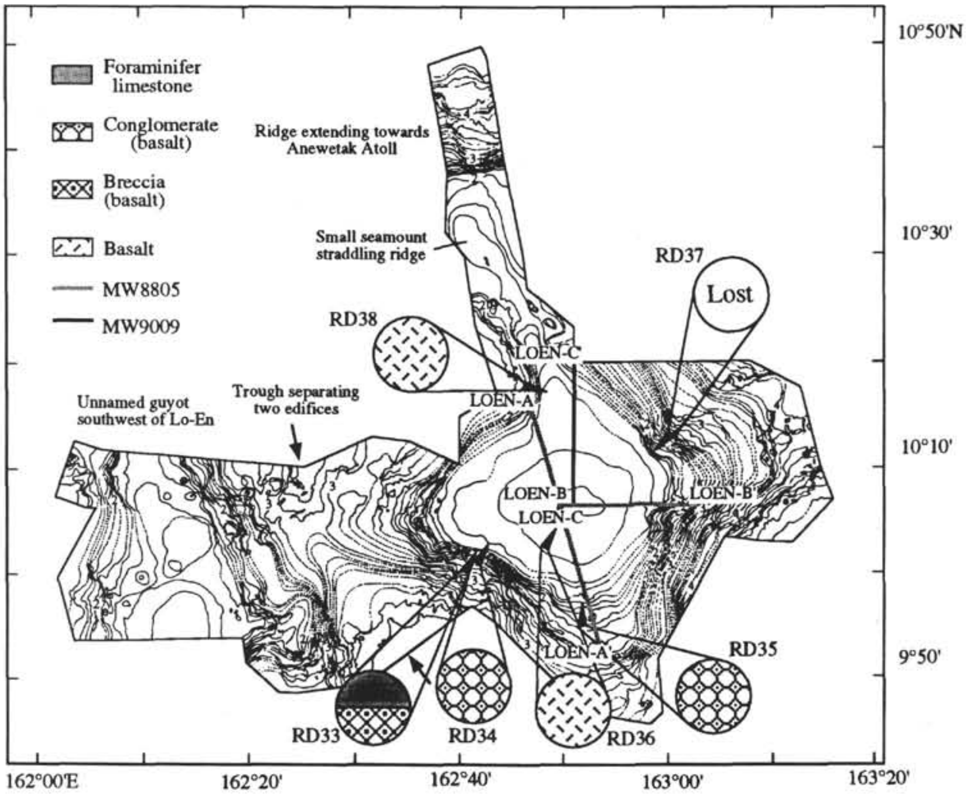

Figure 7. Bathymetric map of Lo-En Guyot. SeaMARC II sidescan sonar and swath bathymetry collected during Cruise MW8805 provided the first detailed coverage over this edifice. The lithology of dredge samples collected during this cruise are superimposed on the SeaMARC II bathymetry (RD = rock dredge). The area shown in the sidescan images (Fig. 7) does not include the small unnamed guyot to the west-southwest of Lo-En. The contour interval is 100 m.

correlation between volcanic rift zones (or elongate zones of volcanism) and other types of ridges extending away from a central edifice (Vogt and Smoot, 1984).

Well-defined ridges connect each of the three atoll and guyot pairs discussed in this paper. On Limalok and Lo-en guyots, these ridges extend from the north-northwest flanks toward Mili and Anewetak atolls, respectively (Figs. 4, 7). The distance between Limalok and Mili (67 km) is comparable to the total size of the two cones forming the island of Tahiti in French Polynesia (65 km; Table 1). Lo-En and Anewetak, on the other hand, are separated by approximately 167 km. High-backscatter features, interpreted as volcanic cones or flows, crop out from the pelagic sediments along the top of this ridge, and a small seamount straddles the ridge at about its mid-point (Figs. 8, 9). A second, smaller ridge extends ~14.5 km from the south flank of Lo-En, its crest plunging away from the edifice at an average of 6° (Table 2). High-backscatter features also crop out from the pelagic sediments along the top of this ridge, forming what appears to be a north-south line of volcanism across the summit of Lo-En (Figs. 8, 9).

Both the number and the shape of flank ridges on Wodejebato Guyot are distinctly different from those observed on Limalok and Lo-En. Five ridges extend from the main edifice of Wodejebato, with the southeast ridge attaching to Pikinni Atoll over a distance of 64 km (Fig. 11). All the other flank ridges are 11 to 13 km long, but the width and the area of each varies considerably (Table 2). The southern and northern flank ridges form broad shelves that deepen gently away from the summit plateau (inclination <2°). The shelf formed by the northern ridge is relatively featureless in the sidescan images, unlike the southern ridge where high-backscatter, cone- and lobe-shaped features crop out from the thin covering of pelagic sediments (Figs. 12, 13). Bergersen (1993) interpreted these features as a combination of volcanic cones and redistributed summit plateau sediments, as dredges along the distal edges of the ridges recovered only basalt and basalt breccia. The absence of shallow-water carbonates in these dredges suggests that the carbonate platform does not extend out onto the shelves, although more localized accumulations of carbonate sediments may be present. The western flank ridge was only partially mapped in the sidescan images, but it does not appear as wide or as planar as its southern and northern counterparts. Along the northeast flank, a narrow volcanic spur (~1.7 km wide) attaches a 300 m high "hill" to the main edifice (Fig. 11). This particular flank ridge may represent a small seamount connected to the main edifice by volcanic flows and volcaniclastic sediments deposited during the constructional phase of Wodejebato (Bergersen, 1993).

Vogt and Smoot (1984) discuss factors controlling the number and length of flank-rift zones on edifices in the Emperor, Geisha (Japanese), Michelson, Dutton, and Mid-Pacific chains, placing major emphasis on the pressure differential between the magma source and the conduits through which the magma flows for defining a model of seamount evolution. They conclude that the height of the edifice correlates with the length of the rift zones but is independent of the number of rift zones. In Hawaii, volcanoes usually possess only two or three rift zones (Fiske and Jackson, 1972). Recent SeaBeam surveying over Society and Austral hotspot volcanoes (Cheminee et al., 1989; Stoffers et al., 1989; Binard et al., 1991) shows five to eight flank ridges extending away from these edifices over distances of up to 20 km; however, it is debatable whether all these ridges are true rift zones with only topographic data as evidence. Until corroborating data (e.g., samples from dredging, modeling of gravity over the ridges) show that the plumbing systems of volcanoes formed in French Polynesia behave differently than those in Hawaii, it seems reasonable to assume that a two or three rift-zone system applies to the shield volcanoes forming the Marshall Islands. In this case, Limalok and Lo-En are simple shield volcanoes. Even though the atoll-linked ridges extending from the north flanks of Limalok and Lo-En and the southeast flank of Wodejebato probably do not represent true rift zones (they more likely result from an accumulation of volcanic

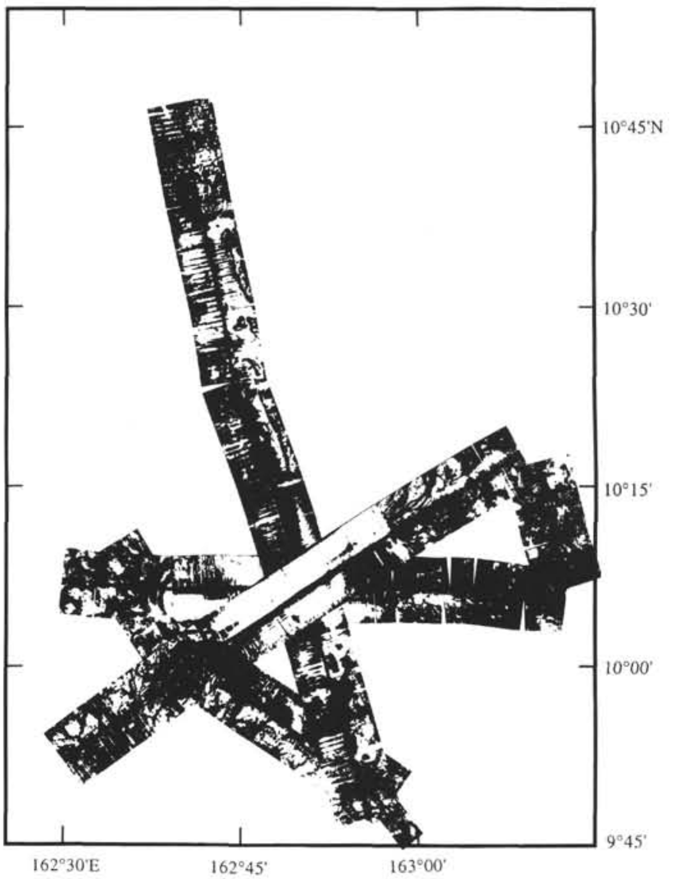

Figure 8. Sidescan images over Lo-En Guyot show a number of high-backscatter, cone- and lobe-shaped features cropping out from the pelagic sediments covering the summit plateau (see Fig. 9 for the location of these features). Relatively small-scale terraces lie perched along the southwest portion of the edifice, and a flank ridge extends to the south.

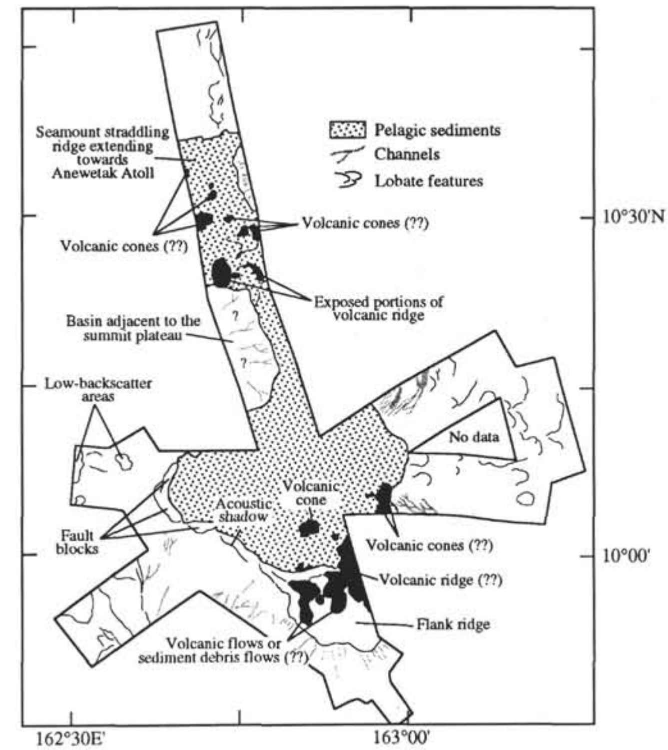

Figure 9. Geologic interpretation of sidescan images over Lo-En Guyot showing the major geomorphic features as related to their backscatter characteristics.

flows and volcaniclastic sediment shed from the two volcanoes during their shield-building stages), the ~100 km difference in length for the Anewetak–Lo-En pair suggests a slightly different volcanic history. The closer spaced atoll-guyot pairs of Pikinni-Wodejebato and Mili-Limalok are more similar to the twin volcanoes forming such islands as Maui in the Hawaiian Chain and Tahiti in the Society Chain. The small size of Wodejebato Guyot argues against this edifice being the product of more than one volcano, and it is more likely that some of the flank ridges on this guyot are not true rift zones (e.g., the western and northeastern flank ridges).

Terraces

Terraces or benches observed in seismic profiles along the flanks of guyots traditionally have been thought to be wave-cut features related to relative lows in sea level (e.g., Pratt, 1963; Budinger, 1967). Sidescan sonar images and swath bathymetric maps often show that the lateral extent of these benches is discontinuous around the edge of an edifice (e.g., Lonsdale et al., 1972; Bergersen, 1993). On the south flank of Wodejebato, sidescan images show that a low-backscatter terrace separates the edge of the carbonate platform (high-backscatter band) from the guyot flank (Fig. 14). Seismic profiles show that flat-lying lagoonal sediments crop out along this scarp, as opposed to truncating against a perimeter ridge present along much of the summit plateau. Vertical displacement of reflectors can also be seen inboard of the main fault scarp. The good correlation between the seismic stratigraphy of the plateau sediments and that of the terrace sediments led Bergersen (1993) to interpret the low-backscatter terrace as a downdropped block of lagoonal sediments.

Observations over Limalok and Lo-En guyots provide additional support for the hypothesis that mass-wasting continues to affect volcanoes after they have moved away from the hotspot swell. For example, on Limalok Guyot arc-shaped terraces (visible in sidescan images) lie outside of the high-backscatter band marking the exposed edge of the carbonate platform (Figs. 5, 6). Seismic profiles across these terraces show large fault blocks downdropped relative to the summit plateau (Figs. 15, 16). In some cases (Fig. 16), the fault block is crossed at an oblique angle, resulting in the appearance of a "ridge" outside of the downdropped block. The resolution of the single-channel data, much poorer than the six-channel data over Wodejebato, makes direct correlation between fault-block stratigraphy and that of the adjacent platform carbonates difficult, but sidescan images show that the blocks are discrete, discontinuous features along the edge of the guyot and hence not wave-cut features. The scarps adjacent to the fault blocks range from 75 to 150 m high. Similar to Wodejebato, smaller scale faulting disrupts the platform carbonates landward of the downdropped blocks. On Lo-En Guyot, the low-backscatter terraces visible in sidescan images along the west flank (Figs. 8, 9) are presumably fault-related as displacements in seismic reflectors can be seen across the more central portions of the summit plateau (Figs. 17, 18). Consequently, mass-wasting of this sort is not unique to edifices capped by shallow-water carbonate platforms, although the size of the fault blocks may be smaller (Table 2).

The paucity of sidescan sonar data and detailed bathymetric maps over submerged islands in French Polynesia prohibits a direct comparison with the fault blocks observed in the Marshall Islands. Given that well-documented, large-scale landslides occur off the islands of Hawaii (Moore et al., 1989), and that similar faulting (and presumably landslide generation) appears common throughout the subaerial islands of French Polynesia (e.g., Moorea and Huahine islands; Table 1), a continuation of this mass-wasting process seems the most likely

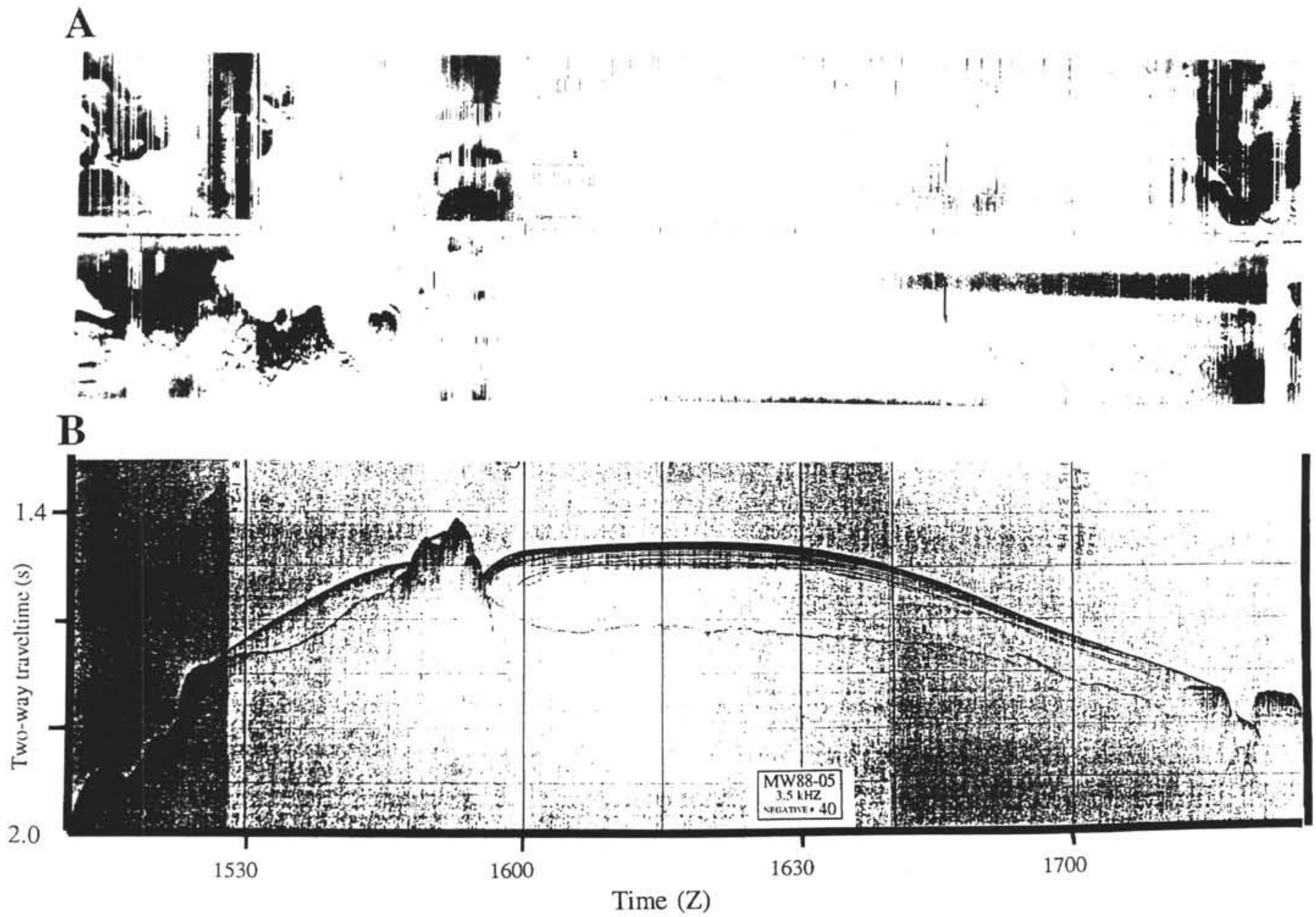

Figure 10. Sidescan image (**A**) and echo sounder profile (**B**) across the summit plateau of Lo-En Guyot. Cruise MW8805 crossed directly over one of the high-backscatter, cone-shaped features shown in the sidescan images. In the 3.5-kHz echo sounder profile, the cone shows a summit depression filled with pelagic sediments. The magnetic high over this cone and the basalt breccia recovered in RD36 suggests that it is volcanic in origin.

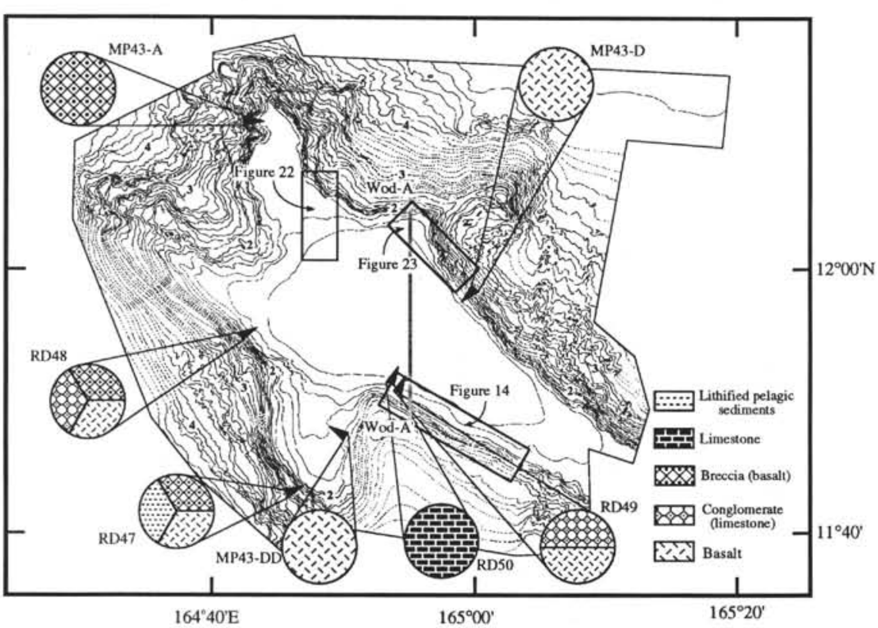

Figure 11. Bathymetric map of Wodejebato Guyot. Location and lithology of dredge samples collected during Cruise MW8805 (RD) and the Mid-Pac Expedition (MP) are superimposed on SeaMARC II bathymetry. Lincoln et al. (1993) used the fossil components of RD50 to help build their model for a mid–Late Cretaceous evolution of the Marshall Islands. The bathymetry clearly shows the five flank ridges extending from the central edifice. Note that the northeast ridge consists of a topographic high detached from the main edifice. The contour interval is 100 m.

Figure 12. Sidescan images over Wodejebato Guyot show a high-backscatter band slightly inset from the edge of the summit plateau. As in the case of Limalok, this band marks areas where the carbonate platform crops out from the overlying pelagic sediments. A second high-backscatter band appears along the shelves formed by the north and northeast flank ridges and the ridge extending toward Pikinni Atoll. In multibeam bathymetric maps and seismic profiles, these bands appear as topographic highs.

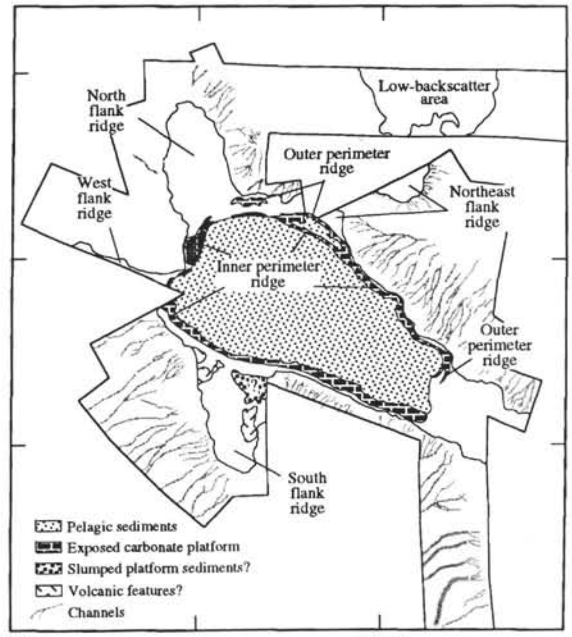

Figure 13. Geologic interpretation of sidescan images over Wodejebato Guyot showing the major geomorphic features as related to their backscatter characteristics.

mechanism responsible for the interpreted fault blocks perched along the flanks of Marshall Islands guyots. The timing and triggering mechanisms of the faulting remain less clear. The faulting evidently happened after the growth of the carbonate platform, as these sediments are part of the fault blocks. One possible cause is sediment overburden as supplied by the carbonate platform lying on top of a clay weathering horizon. Another possibility is that the volcanic flows and volcaniclastic sediments forming the original shield volcano are inherently unstable and therefore susceptible to failure in response to local seismic activity (e.g., Walker and McCreery, 1988). Mass wasting of this sort indicates that the stability of edifices away from the hotspot swell remains poor.

Summit Plateau

As mentioned previously, one of the keys to reconstructing a Cretaceous sea-level curve based on the sediments drilled during Leg 144 is the separation of sea-level fluctuations of a eustatic origin from those brought about by such local tectonic forces as plate uplift and plate flexure. The sequences of sediment sampled across the summit plateaus of Limalok, Lo-En, and Wodejebato represent our best record of the sum effects of volcanism, uplift, and subsidence. Consequently, the first step toward removing, or at least better understanding, the tectonic sea-level signal associated with these guyots is to examine the topography and architecture of the summit plateaus.

Drilling at Site 872 on Lo-En Guyot encountered no platform limestones or clay transition zone between the basalt flows and overlying pelagic sediments, although preliminary interpretations of the seismic and dredge data predicted at least a thin sequence of platform carbonates. Basalt units sampled at Hole 872B suggest that the flows forming the volcanic platform represent the very latest shield stage or alkalic-cap stage of hotspot volcanism, and probably were erupted subaerially (Christie et al., this volume). Biostratigraphic data from Site 872 indicate that a long hiatus (>50 m.y.) occurred between the late Oligocene to Pleistocene pelagic sediments and the pre-Turonian volcanic platform (Premoli Silva, Haggerty, et al., 1993). Given the results of drilling at Site 872, the reflectors within single- and six-channel seismic profiles across Lo-En may be interpreted as volcaniclastic or igneous material beneath the pelagic cap rather than as platform carbonates (Figs. 17, 18). No fringing reef buildups are visible in the six-channel data (Fig. 18) although Profile A–A′ crosses a mound or perimeter ridge along the north edge of the summit plateau (Fig. 17). On the basis of the high magnetic signature and the basalt breccia recovered from the cone surveyed during Cruise MW8805 (RD36), other cone- and lobe-shaped features visible in the sidescan images (Fig. 8) appear to be volcanic in origin; hence, the "perimeter ridge" in Profile A–A′ may also be igneous rather than sedimentary. The volcanic cone sampled by Dredge RD36 is roughly the size of Diamond Head, a well-known post-erosional cone in the Hawaiian Islands. Unfortunately, the high degree of alteration of the breccia recovered in Dredge RD36 precludes any detailed interpretation of the cone's age or origin (e.g., a tuff cone formed during secondary eruptions, as in the case of Diamond Head). The lack of recovered platform material and the presence of cones across the relatively flat summit plateau contradict traditional views of island evolution in which slow plate subsidence allows edifice truncation and shallow-water carbonate accumulation. Lo-En must have subsided at such a rate, or been constructed at such a latitude, that extensive weathering of the volcanic platform and reef growth across the summit plateau were prohibited. Alternatively, the volcanism responsible for the cones could have occurred in a submarine environment, thus circumventing subaerial erosion.

The stratigraphic units drilled on the submerged carbonate platforms of Wodejebato and Limalok are similar to those observed on uplifted or drilled atolls in French Polynesia. For example, Rurutu Island in the Austral Chain is an uplifted, deeply dissected shield volcano with younger flows (1–2 m.y.) superimposed on an older edifice (8.6–12.5 m.y.; Turner and Jarrard, 1982). Shallow-water carbonate sediments form 90- to 100-m high cliffs around the entire island, and a 3-m-thick stratified layer of clay marks a transition zone between the volcanic and limestone units (Duncan and McDougall, 1976; Bardintzeff et al., 1985). This stratigraphic sequence resembles the sequence of sediments drilled at Site 873 on Wodejebato Guyot,

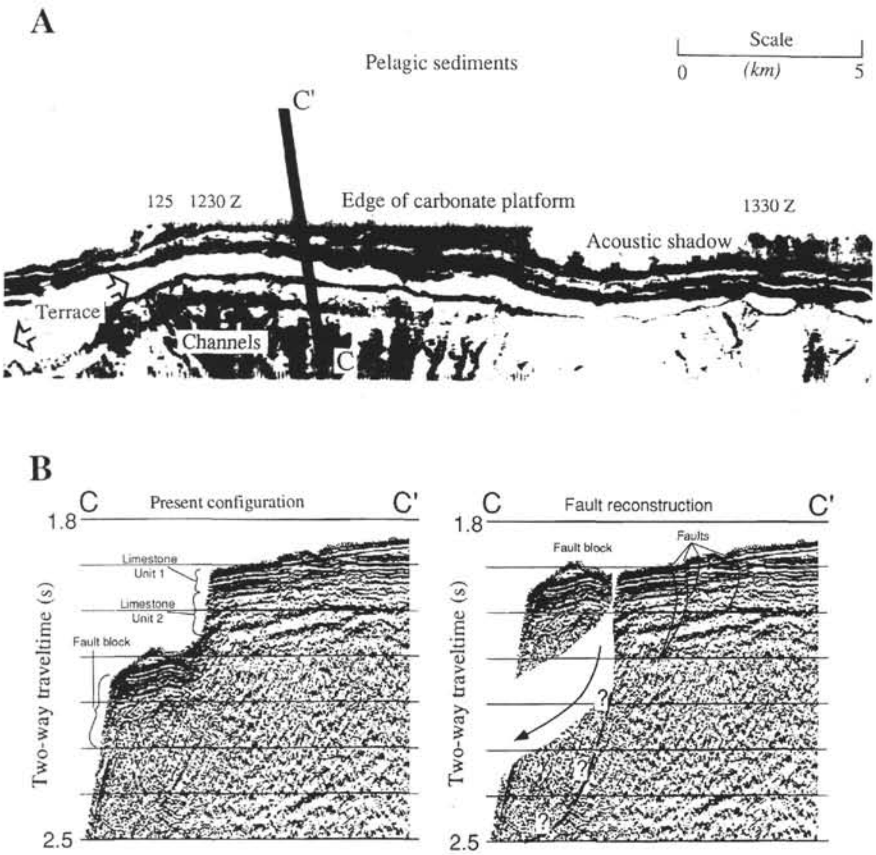

Figure 14. Low-backscatter terrace visible in the sidescan images along the south flank of Wodejebato (**A**) appears as a fault block in migrated six-channel seismic data (**B**). The seismic stratigraphy of the fault block matches that of the lagoon sediments. Faulting also appears to disrupt the carbonate platform farther back from the edge of the summit plateau. Sidescan image location is shown in Figure 11.

although the transitional clay layer at this site is much thicker (20 m). The clay transition zone is also much thicker on Limalok Guyot at Site 871 (30 m). Drilling on Muruoa Atoll in the Gambier-Pitcairn Chain provides another example of how the French Polynesian islands are similar to the volcanic platforms beneath Wodejebato and Limalok (Table 1). Muruoa Atoll was extensively sampled through drilling along an east-northeast transect (Buigues, 1985). The depth at which these drill holes encountered basalt shows that the top of the volcanic substrate shoals toward the center of the summit plateau. In a similar fashion, the thickness of the carbonate platforms on Limalok and Wodejebato increase toward the edges of their summit plateaus (Fig. 19). On Limalok, the seismic basement high traverses the central portion of the summit plateau, possibly merging with the ridge extending toward Mili Atoll. On Wodejebato, the seismic basement high appears to consist of two separate peaks offset to the northeast, although these peaks may be an artifact of widely spaced seismic profiles. Seismic profiles over both Limalok and Wodejebato show major subunits within the carbonate platform onlapping these central seismic basement highs (e.g., Figs. 20, 21; also see discussion by Arnaud et al., this volume).

In modern atoll environments, a raised reef rim encircles a central lagoon, commonly dotted with patch reefs and small islands. Relief across the top of the submerged platforms of Wodejebato and Limalok (5 and 10 m) is typical of depth ranges for the lagoons in most atoll settings (e.g., Weins, 1962), but the presence of a reef rim is not clear in most cases. On Wodejebato, two ridges appear in the sidescan images along the north and northeast flank ridges, and along the ridge extending toward Pikinni Atoll (Fig. 22; see also Bergersen, 1993, fig. 7). The inner ridge is the more continuous of the two, appearing in all seismic profiles except those across the south flank (Bergersen, 1993). A similar ridge on Limalok is shown only in seismic data along the eastern and northern sides of the summit plateau (Fig. 16; see also Premoli Silva, Haggerty, Rack, et al., 1993, fig. 5). Given the amount of mass-wasting affecting these platforms, it would not be surprising if such features have been eroded from the various margins.

Summary

From a geomorphic and stratigraphic perspective, the volcanic edifices and carbonate platforms of the guyots drilled during Leg 144 in the Marshall Islands share a number of similarities with modern islands and atolls in the Hawaiian and French Polynesian chains. The interpreted mass-wasting along the flanks of the guyots suggests that the edifices remain unstable even after moving away from the hotspot swell, although the triggering mechanism for this faulting and the depth to which the faults extend remain unclear. If the faults only affected the carbonate platform (being listric in nature, and thereby soling in the clay unit separating the carbonates from the volcanics), one would expect to see backtilting of the blocks as they rotated along the fault plane. This does not appear to be the case on Wodejebato and Limalok guyots (Figs. 14–16), which suggests that the faults extend into the volcanic substrate.

The gross physiography and stratigraphy of the submerged carbonate platforms on Wodejebato and Limalok resembles that of atolls in French Polynesia (e.g., perimeter ridges bounding lagoon sediments, a transition zone of clay and altered volcaniclastic sediments separating the shallow-water platform carbonates from the underlying volcanic flows), which makes the apparent absence of a carbonate platform across the summit plateau of Lo-En all that more intriguing. Given the complicated history of volcanism, uplift, and subsidence displayed by many French Polynesian edifices (e.g., Rurutu, Makatea, Mauke, Mitiaro), it is no wonder the guyots in the Marshall Islands display such a wide variation in morphology and stratigraphy. The 230-m-thick Paleocene to middle Eocene carbonate platform of Limalok, the 100-m-thick Late Cretaceous carbonate platform of Wodejebato, and the cone-riddled summit plateau of Lo-En all record a different history of subsidence after the main stage of volcano construction. In the next two sections, I address the effects of plate flexure, thermal subsidence and edifice size on platform development and demise.

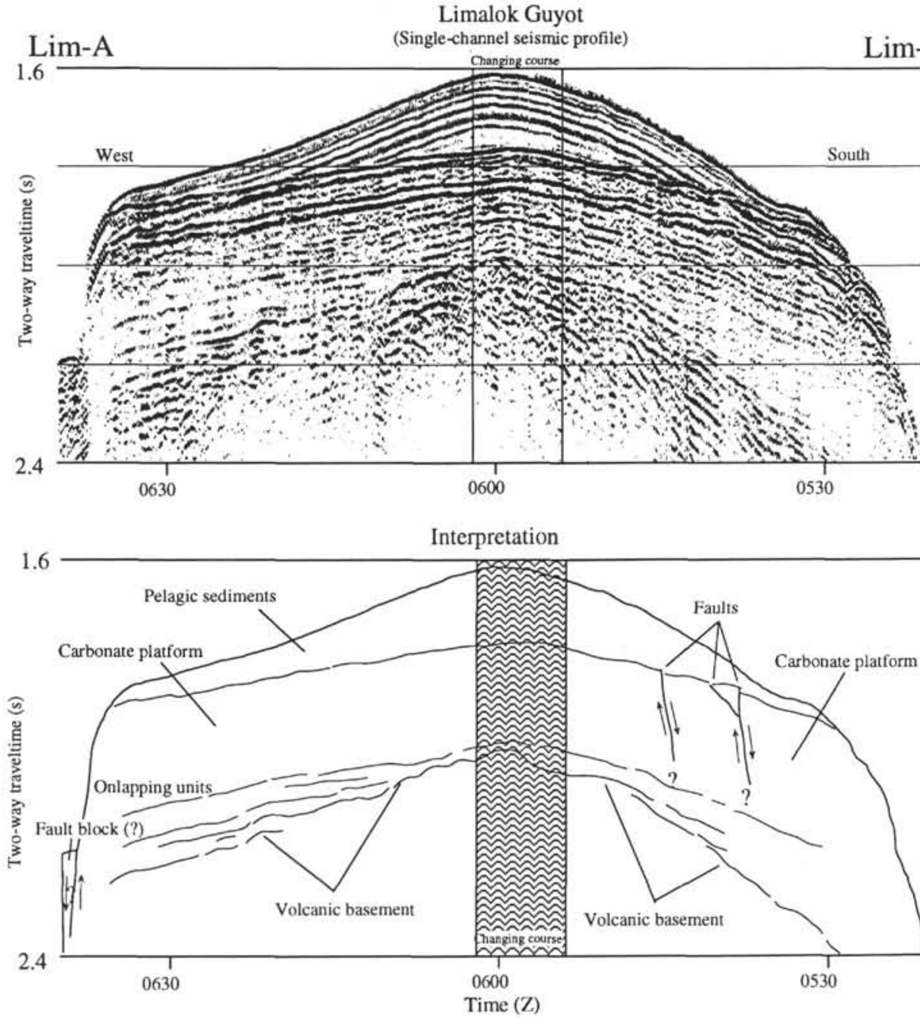

Figure 15. The faulting noted on Wodejebato Guyot also occurs on the south and west flanks of Limalok Guyot, although this profile only shows a small portion of the faulting along the west flank (left side of figure). Smaller faults offset platform reflectors along the south flank. Platform reflectors onlap the seismic basement reflector; the poor quality of the records precludes a more detailed interpretation of the guyot's internal structure. Profile location is shown in Figure 4.

PLATE FLEXURE AND PLATFORM DEVELOPMENT

During construction of a volcano, the plate flexes in response to the new load. The moat and arch around the load cause subsidence and uplift on the adjacent seafloor (e.g., McNutt and Menard, 1978; Watts and ten Brink, 1989). The magnitude and rate of flexure can be quite pronounced. For example, flexure modeling for the island of Hawaii suggests that the moat formed by this load depressed the island of Maui by 1000 to 2000 m (Watts and ten Brink, 1989). As the average construction time of a Hawaiian-type volcano is ~0.5 m.y. (Moore and Clague, 1992), the average rate of subsidence on Maui was at least 1 to 2 mm/yr during the time of loading, or near the maximum rate of carbonate accumulation for modern reef systems. Hence, plate flexure from volcanic loading is an appealing mechanism for explaining relatively rapid changes in sea level observed on platforms (e.g., tilting of seismic basement reflectors or plateau tops, submergence or emergence surfaces on carbonate platforms) and may be responsible for rejuvenescent volcanic events on existing islands as tensional stresses and uplift occur in the arch region.

Observations from French Polynesia are once again a key to understanding and modeling plate flexure in the Marshall Islands. McNutt and Menard (1978) present a flexure model that explains not only the observed uplift on ancient volcanic islands and atolls in the Cook, Tuamotu, Marquesas, and Pitcairn groups but also provides a good estimate of flexural rigidity for the plate in this region (1.7 to 2.5 $\times 10^{22}$ N m). As a whole, their model fits the observed data (primarily uplifted islands) quite well, although some of the model parameters may require adjustment. For example, although Jarrard and Turner (1979) agree that plate flexure plays an important role in the uplift of the French Polynesian islands, they argue that McNutt and Menard (1978) underestimate the amount of uplift on various atolls and oversimplify the episodes of volcanism affecting these island chains. Such observations serve as a warning toward attempting flexure modeling in the Marshall Islands, where age data are more scarce and the episodes of volcanism are even less understood. The primary focus of this section is to define the wavelength and, to a lesser degree, the amplitude of flexure caused by construction of selected volcanoes, in particular those beneath the atolls of Anewetak and Pikinni on adjacent edifices. The paucity of information relating to the volcanic and erosional history of edifices within this region limit the modeling to showing the areas over which relative deformation occurred (Fig. 23).

Anewetak and Lo-En

Anewetak and Lo-En exhibit the best age controls of the three atoll and guyot pairs discussed in this paper. Drilling results from these edifices show that construction of Lo-En occurred at ~113 Ma,

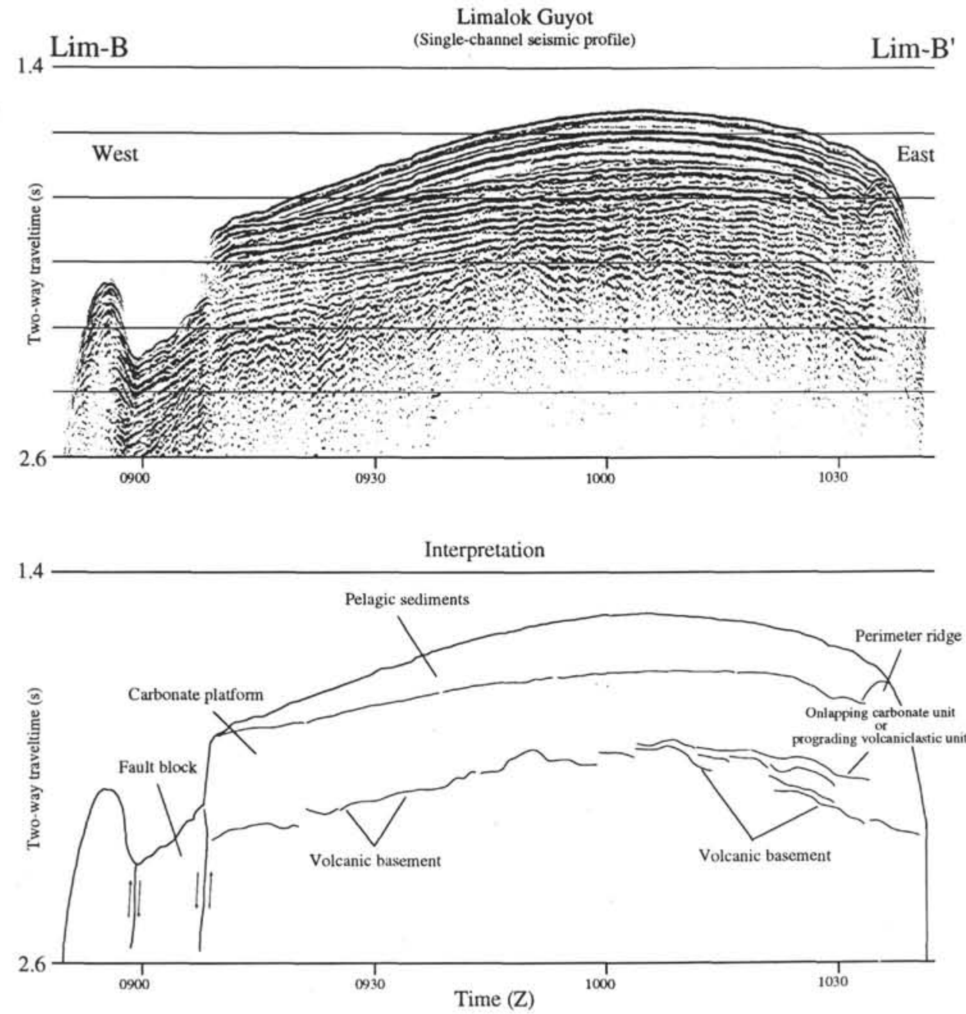

Figure 16. Single-channel seismic profile showing one of the terraces seen in the sidescan images along the west flank of Limalok Guyot. A large fault block lies downslope from the edge of the carbonate platform. The faulting along the flanks of this guyot produces a scalloped appearance to the summit plateau. This particular seismic profile crossed one of the fault blocks at an oblique angle; hence, a topographic high appears outside of the block as the ship passed over a portion of the plateau unaffected by the faulting. Note what appears to be a perimeter ridge bounding the east side of the plateau. As in the case of Profile A–A′, some of the platform reflectors onlap the basement reflector. Profile location is shown in Figure 4.

whereas construction of Anewetak was at ~76 Ma (Pringle, 1992; Premoli Silva, Haggerty, Rack, et al., 1993; Pringle and Duncan, this volume). As shown by Figure 23A, Lo-En lies squarely in the region of 0 deflection produced from loading on Anewetak. If the 10-km plate thickness is more accurate, then Lo-En should have been sitting on the flexural arch of Anewetak. Conversely, if the 20-km plate thickness is more correct, then Lo-En should have subsided up to 100 m and the summit plateau should be tilted toward Anewetak.

The depth to the top of the volcanic substrate for these two edifices is approximately equal; drilling along the perimeter of Anewetak reached basalt between 1283 and 1410 m, and drilling at Site 872 on Lo-En encountered basement rocks at ~1225 m. The platform beneath the pelagic sediments tilts slightly in the direction of Anewetak, increasing in depth from 1267 m on the south side to ~1305 m on the north side (Fig. 10). Hence, it appears Lo-En was located on the moat side of the flexural arch formed during construction of Anewetak. Now, how does this flexure hypothesis relate to the observed abundance of cone- and lobe-shaped (volcanic) features and interpreted paucity of platform carbonates across the summit plateau of Lo-En? If Menard's (1983) estimate for the rate of shelf widening in the Marquesas and Hawaiian islands (1.1–1.7 km/m.y.) accurately measures the rate at which volcanic islands were truncated during the Cretaceous in the Marshall Islands, then Lo-En should have been eroded to sea level 6–10 m.y. after its formation, well before eruptions at Anewetak took place. Magnetic inclination data suggest this edifice formed around 30°S (Nakanishi et al., 1992a), near the present-day limit for active coral growth (Grigg, 1982). Even though plate motion was carrying the volcano into latitudes more favorable for reef growth, an extensive carbonate platform apparently did not accumulate across the summit plateau. The apparent absence of a "reef" rim might explain the overall flatness of Lo-En's summit plateau (no barrier to prevent erosion across the interior of the plateau) but argues against the survival of the topography cropping out from the pelagic sediments. Presumably, Late Cretaceous uplift occurred across Lo-En as it passed over the hotspot swell associated with the formation of Anewetak. The flexure modeling presented here suggests that Lo-En may have subsided slightly as a moat formed around Anewetak; in this case, minor subsidence (flexure) was superimposed on the regional uplift (hotspot swell). Such subsidence may have been sufficient to prevent the truncated summit from reaching a depth where Late Cretaceous or early Tertiary reefal organisms could successfully colonize the volcanic platform, as is the case for Anewetak (hence, no carbonate platform was established on Lo-En). Conversely, stresses associated with formation of the flexural arch may have been respon-

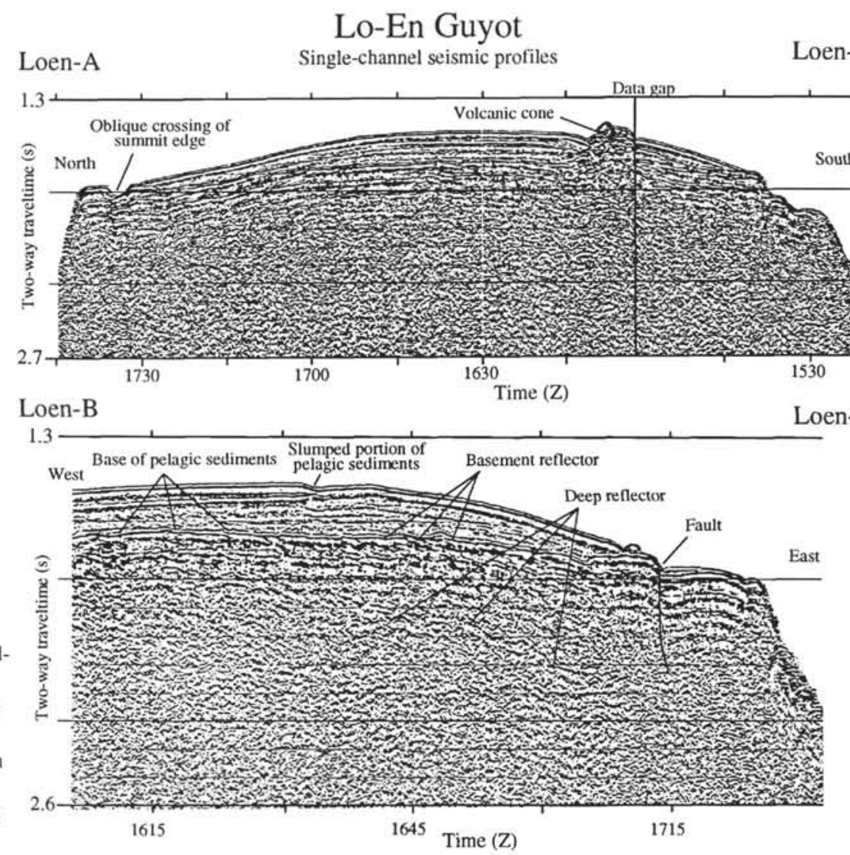

Figure 17. The nature of the sediments beneath the pelagic cap of Lo-En were unclear from the single-channel seismic profiles collected during Cruise MW8805. Profile A–A′ shows the presumed volcanic cone that crops out from the pelagic sediments, and Profile B–B′ is a portion of the seismic line from which Site 872 was originally selected. On the basis of the drilling results at Site 872, an extensive carbonate platform is apparently absent across the summit plateau. Faulting appears to offset reflectors across the plateau. The deep reflector annotated in Profile B–B′ was first identified in migrated six-channel data (see Fig. 18) and suggests a change in the character of the volcanic substrate. Profile location is shown in Figure 7.

sible for a second phase of volcanism across Lo-En's summit plateau, thus explaining the cones cropping out from the pelagic sediments.

Pikinni and Wodejebato

Age controls on Wodejebato are quite good; unfortunately, the same is not true for Pikinni. Nannofossils within the clay unit at Site 873, along with the volcaniclastics recovered from the archipelagic apron hole at Site 869, suggest that the original shield volcano forming Wodejebato was constructed during the Cenomanian (~95 Ma; Erba and Watkins, this volume), whereas all the $^{40}Ar/^{39}Ar$ dates from the basalt units produce an average age for volcanism of 83.2 ± 1.1 m.y. (Pringle and Duncan, this volume). Carbonate platform demise on Wodejebato occurred in the middle Maastrichtian (~70 Ma; Premoli Silva et al., this volume).

Drilling during Operation Crossroads on Pikinni sampled Eocene platform carbonates but failed to reach the underlying volcanic substrate. The model shown in Figure 23B assumes that Pikinni was constructed at about the same time as Anewetak (~76 Ma) and, therefore, that flexure from this load affected the existing edifice of Wodejebato. This assumption essentially tests whether plate flexure was responsible for the demise of the carbonate platform on top of Wodejebato. Figure 23B shows that if Pikinni was constructed after Wodejebato, it would lie within the moat of Pikinni (slightly inside the 300 m region of downward deflection). Seismic profiles across the summit plateau of Wodejebato show no pronounced tilting to the southeast of either the top of the carbonate platform or the seismic basement reflector. In fact, the opposite appears true; seismic basement tends to shallow to the northeast (Fig. 21). Flexure modeling also suggests that the basement depth on Wodejebato should lie at least 300 m deeper than that on Pikinni (Fig. 23B). Although Raitt (1954) estimated that the average depth to the top of the volcanic substrate on Pikinni is ~1300 m, the data support a depth range between 600 and 2100 m. Depth to the top of the volcanics at Site 873 is 1509 m, but this site lies southwest of the seismic basement high. Hence, it is difficult to prove whether an appreciable difference exists between the depths to the volcanic substrate of these two edifices.

Given the poor age and depth controls on the volcanic platform of Pikinni, another possibility is that Wodejebato is younger than Pikinni. Such a scenario does not appear likely because additional subsidence on Pikinni would hinder the survival of its carbonate platform during the event responsible for the demise of Wodejebato. Rather, the model results compared to the observed data suggest that both edifices were built at approximately the same time. Seismic basement reflectors on Wodejebato do not appear to be tilted toward Pikinni, and Pikinni reefs survived the event responsible for the demise of Wodejebato.

Limalok

In a fashion similar to the Pikinni-Wodejebato pair, it is unlikely that construction of the edifice beneath Mili Atoll occurred much later than the edifice beneath Limalok Guyot because neither the top of the carbonate platform nor the seismic basement reflectors of Limalok tilt to the north-northwest. On the contrary, seismic basement reflectors on this guyot fan to the south (Fig. 20). One way to cause such a stratal pattern is to load the plate in this direction (Fig. 23C). The moat formed by the edifice to the south of Limalok encompasses the area occupied by this guyot. If we assume that the plate was moving to the north-northwest at a rate of 10 cm/yr, then the modeled load was constructed ~1–2 m.y. after Limalok. This relatively short period of time is insufficient to account for the growth and demise of the carbonate platform on top of Limalok, but it may explain the fanning sequence of seismic basement reflectors observed across the summit plateau.

Summary

Flexure modeling in the Marshall Islands is subject to a number of assumptions concerning plate and load parameters, the most important being the time of plate loading. The simple models presented in

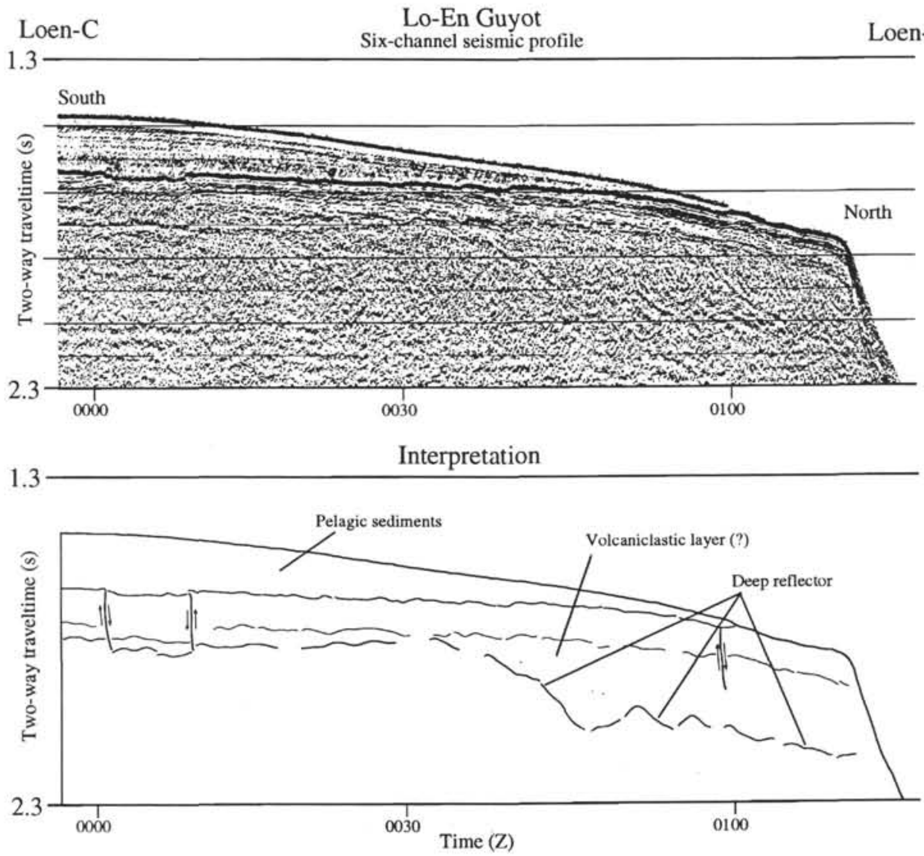

Figure 18. Digital, six-channel seismic data collected during Cruise MW9009 help define the "sub-basement" structure of Lo-En Guyot. The "deep reflector" annotated here is much more apparent than in the single-channel data, although the significance of this reflector is still poorly understood. It may represent some type of flow unit overlain by volcaniclastic sediment. A similar reflector also appears on Wodejebato Guyot. Profile location is shown in Figure 7.

this paper do not answer all the questions concerning the evolution of Limalok, Lo-En, and Wodejebato guyots, although they provide additional insights on the history of volcanism, uplift, and subsidence for this region.

Two observations must be accounted for when discussing the evolution of Lo-En: volcanic cones exist across the relatively flat summit plateau, and reefal organisms failed to colonize this platform during the Late Cretaceous uplift event associated with Anewetak volcanism. The apparent time lag (~35 m.y.) between volcanism on Lo-En Guyot and Anewetak Atoll is sufficiently long to have allowed complete truncation of the original shield volcano forming Lo-En. Without an apparent protective fringing reef along the edges of the summit plateau, it seems unlikely that any sort of erosional remnant would survive this period of subaerial erosion, unless of course sea level rose rapidly near the time of complete truncation. Regional uplift, probably related to a hotspot swell, almost certainly occurred during the Late Cretaceous volcanic event recorded at Anewetak. Whether this uplift was sufficient to cause subaerial exposure across Lo-En's summit is unknown. The flexure modeling presented in this paper suggests that Lo-En most likely experienced subsidence of up to 100 m as a moat formed around the Anewetak load. Such subsidence may have been sufficient to prevent the truncated summit of Lo-En from reaching a depth where reefal organisms could successfully colonize the volcanic platform, thus explaining the absence of Late Cretaceous or early Tertiary shallow-water carbonates across the plateau. In addition, stresses associated with the plate flexure may have created an easier path for the penetration of magmas on Lo-En, thus producing a second phase of volcanism and explaining the cones cropping out across the summit plateau. Currents associated with a moderately shallow-water environment could presumably erode the clays and other sediments marking the original truncation horizon without affecting the volcanic cones.

Although flexure modeling around Wodejebato and Limalok is less constrained than around Anewetak, it still provides some useful insights into the evolution of these two guyots. The absence of tilted volcanic or carbonate platforms suggests that the original shield volcanoes beneath living atolls and the drowned carbonate platforms were constructed at approximately the same time. Flexure from loading to the south of Limalok may be responsible for the pattern of prograding basement reflectors seen in the seismic profiles across this guyot.

The simple models presented in this paper only describe the flexure associated with the construction of a single volcano. A more accurate model would incorporate the flexure associated with other nearby volcanoes, but the poor age controls on these edifices prevent such an analysis. For example, although it appears that Pikinni and Wodejebato were constructed at approximately the same time, loading on adjacent edifices (e.g., the Ronlap atoll complex) may have resulted in additional episodes of uplift or subsidence across these two edifices.

THERMAL SUBSIDENCE, EDIFICE SIZE, AND PLATFORM DEMISE

The demise of a carbonate platform occurs when the rate of relative sea-level rise exceeds the rate of net carbonate accumulation and subsequent falls in sea level fail to bring the carbonate bank up to a depth where the accumulation rate can once again keep pace with changes in sea level. As a plate moves away from a ridge or hotspot, thermal cooling of the plate results in subsidence that adheres to a $(\text{time})^{1/2}$ relationship for plates less than ~70 m.y. (Parsons and Sclater,

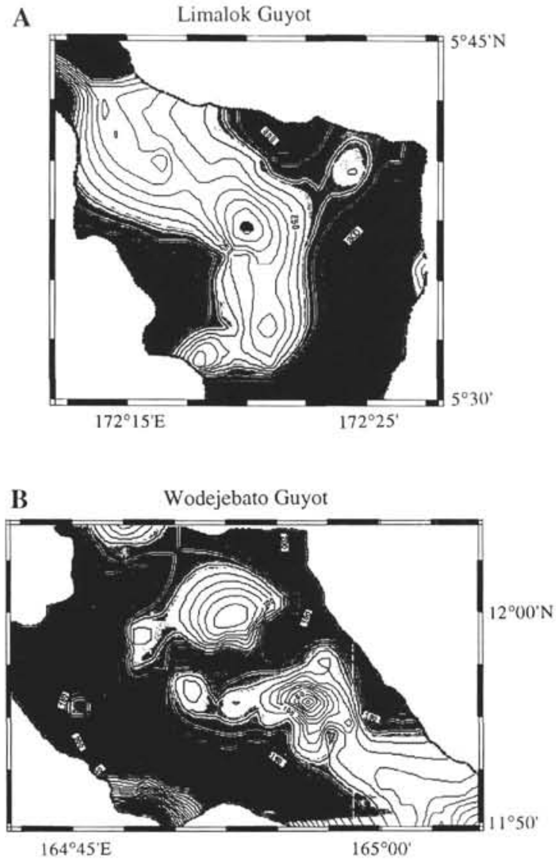

Figure 19. Isopach maps of carbonate platform thickness constructed from the seismic profiles over Limalok (**A**) and Wodejebato (**B**) guyots show that the platforms thicken toward the margins of the summit plateau. The maps were generated by subtracting a grid of pelagic-platform reflector depths from a grid of platform-basement reflector depths; and the thicknesses shown here are in milliseconds. Thick gray lines represent the contour approximately marking the edge of the summit plateau (1600 m on both guyots). In this figure, the isopach contours truncate against this bathymetric contour, whereas in reality the isopach contours should converge to 0 at the edge of the platform. As the top of the carbonate platforms are essentially horizontal, changes in platform thickness represent changes in volcanic substrate topography. Consequently, these isopach maps show the configuration of the seismic basement reflector noted in various profiles. The seismic basement high on Limalok Guyot merges with the ridge extending toward Mili Atoll (to the north), whereas the seismic basement high on Wodejebato Guyot appears offset to the northeast across the summit plateau. The two peaks in seismic basement on Wodejebato Guyot probably result from the wide spacing of ship tracks.

1977). Observations of subsidence rates on portions of plates passing over hotspots in comparison to portions of equal age unaffected by hotspots suggest that the former subside at anomalously fast rates by way of resetting the thermal age of the plate to some value less than its absolute age (Detrick and Crough, 1978; Crough, 1983a). A number of authors have shown that plate subsidence in response to thermal cooling is an unsatisfactory explanation for the demise of modern platforms because the rates are generally too slow (e.g., Wilson, 1975; Schlager, 1981; Grigg and Epp, 1989). For example, if the thermal age of a plate was reset to 25 m.y. for a plate passing over a hotspot (Detrick and Crough, 1978), the initial subsidence of the plate (and newly formed volcano) approaches 0.035 mm/yr. This rate is more than an order of magnitude less than the maximum rate of net sediment accumulation for modern reef systems (those composed of scleractinian corals, ~1–10 mm/yr; e.g., Buddemeir and Smith, 1988). The shallow-water carbonate sediments on the Marshall Islands guyots probably accumulated at a slower rate than modern reef systems because the Cretaceous "reefs" are composed of organisms other than scleractinian corals (e.g., rudists). Camoin et al. (this volume) estimate a total accumulation rate of ~60 m/m.y. (0.06 mm/yr) for the platform on top of Wodejebato, but this estimate does not account for sediment lost to erosion (platform exposure) and probably does not reflect the maximum growth potential for the carbonate producing organisms. Hence, I doubt thermal subsidence was the primary cause for platform demise (see also Larson et al., this volume; and Arnaud et al., this volume).

In the Hawaiian chain, Grigg and Epp (1989) showed that in most cases islands possessed larger summit areas than submerged platforms, leading them to postulate that the size of the summit plateau plays an important role in determining the survival or demise of coral islands. Edifice size in the Hawaii case is inversely related to the truncation depth. During a low sea-level stand, wave erosion acts more quickly to reduce smaller edifices to sea level than larger ones. During subsequent rises in sea level, the truncated platforms may be submerged to such a depth that coral growth rates are insufficient to allow a successful recolonization. After the Holocene transgression, the smaller platforms in the Hawaiian chain were too deep for coral growth to keep pace with tectonic subsidence, whereas incompletely truncated edifices provided a portion of the platform shallow enough for coral organisms to recolonize and survive. This model is consistent with the observed carbonate bank development on the Great Barrier Reef in Australia where Holocene reefs grow primarily on top of antecedent Pleistocene topography (e.g., Hopley, 1982).

The volcanic platforms associated with the atoll and guyot pairs discussed in this paper generally adhere to the Grigg and Epp (1989) model: platforms beneath living atolls are larger than submerged platforms. However, the degree to which differences in summit area explain all submerged carbonate platforms in the Marshall Islands is debatable because of the apparently complicated volcanic, uplift, and subsidence history of these edifices (Lincoln et al., 1993; Bergersen, this volume), and the relatively sparse mapping in this area (and hence accurate measurements of volcanic platform size and depth). Without additional samples and age controls on surrounding edifices, the ultimate cause of platform failure can not be determined (e.g., cooler sea-surface temperatures, more nutrient-rich waters, rapid subsidence in response to plate flexure).

CONCLUSIONS

Limalok, Lo-En, and Wodejebato guyots are all comparable in some respects to modern islands and atolls in French Polynesia, and this area of the Pacific holds perhaps the most promise for understanding the tectonic environment responsible for the formation of edifices within the Marshall Islands. A good understanding of the volcanism and tectonism affecting the Marshall Islands is crucial for any attempt to establish a eustatic sea-level curve from the sediments cored during Leg 144. It is clear from the data presented in this paper that simple plate subsidence does not explain all the features noted across the summit plateaus and along the flanks of Limalok, Lo-En, and Wodejebato.

Plate flexure associated with volcano construction has influenced the history of uplift and subsidence experienced by edifices within the Marshall Islands; however, with the paucity of age data from the various island groups, only simple models can be constructed showing relative regions of arching or downwarping. The flexure models presented here may explain the negligible difference between the volcanic substrate depths of Anewetak and Lo-En, the high-backscatter, cone- and lobe-shaped features cropping out along the flat summit plateau of Lo-En, and the prograding sequence of basement reflectors on Limalok. The models also suggest that construction of the volcanic platforms beneath Wodejebato and Pikinni, and possibly Limalok and Mili, occurred without a substantial gap in time. Plate flexure does not appear to be the cause of carbonate platform demise on Wodejebato or Limalok, but it may have influenced depositional patterns during

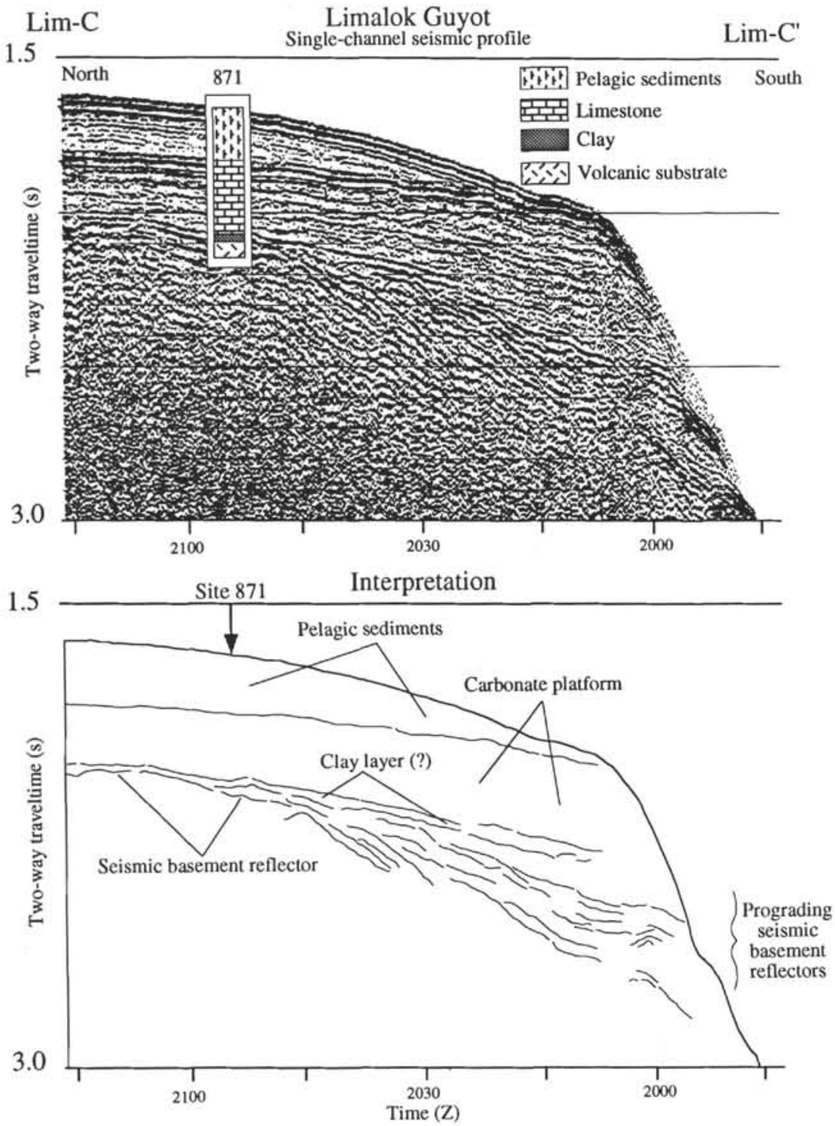

Figure 20. Single-channel seismic data collected during Leg 144 over Limalok Guyot shows the internal structure of the carbonate platform. Basement reflectors fan toward the south. Small-scale faulting appears to offset reflectors across the summit plateau. Profile location is shown in Figure 4.

the early stages of platform development. If carbonate islands in Hawaii are indicators of how some platforms fail, then summit plateau areas may have played substantial roles in the survival of Anewetak, Pikinni, and Mili atolls. Undoubtedly, the local environmental conditions (e.g., sea surface temperature, nutrient content) were also important (Larson et al., this volume).

A better understanding of the evolution of the Marshall Islands requires improved age controls on volcanoes within the various island chains and more rigorous testing of whether these chains display "well-behaved" hotspot trends (e.g., Bergersen, this volume). Until the sequence and timing of volcanism and mass-wasting in the Marshall Islands is better understood, and hence the tectonic signal of sea-level changes can be removed, using drowned carbonate platforms in the Marshall Islands as "dipsticks" for recording the history of Cretaceous sea-level fluctuations requires close examination of the tectonic setting and history.

ACKNOWLEDGMENTS

I thank F. Duennebier, A. Shor, J. Sinton, P. Wessel, and R. Wilkens for discussions concerning the scope of this study. Course notes and computer routines developed by P. Wessel were used to model plate flexure. Critical reviews from P. Vogt, A. Shor, J. Haggerty, and an anonymous reviewer improved the contents of the manuscript. Funding for this research came from National Science Foundation Grant OCE-8709568 and a USSAC Site Augmentation grant.

REFERENCES*

Bardintzeff, J.M., Brousse, R., and Gachon, A., 1985. Conditions of building of coral reefs on a volcano: Mururoa in Tuamotu and Rurutu in Australes (French Polynesia). *Proc. 5th Int. Coral Reef Congr.,* 6:401–405.

Bates, R.L., and Jackson, J.A. (Eds.), 1980. *Glossary of Geology* (2nd ed.): Alexandria, VA (Am. Geol. Inst.).

Bergersen, D.D., 1993. Geology and geomorphology of Wodejebato (Sylvania) Guyot, Marshall Islands. *In* Pringle, M.S., Sager, W.W., Sliter, W.V., and Stein, S. (Eds.), *The Mesozoic Pacific: Geology, Tectonics, and Volcanism.* Geophys. Monogr., Am. Geophys. Union, 77:367–385.

Binard, N., Hekinian, R., Cheminee, J.L., Searle, R.C., and Stoffers, P., 1991. Morphological and structural studies of the Society and Austral hotspot regions in the South Pacific. *Tectonophysics,* 186:293–312.

Blackinton, J.G., 1986. Bathymetric mapping with SeaMARC II: an elevation-angle measuring sidescan sonar system [Ph.D. dissert.]. Univ. of Hawaii, Honolulu.

* Abbreviations for names of organizations and publications in ODP reference lists follow the style given in *Chemical Abstracts Service Source Index* (published by American Chemical Society).

Buddemeir, R.W., and Smith, S.V., 1988. Coral reef growth in an era of rapidly rising sea level: predictions and suggestions for long-term research. *Coral Reefs,* 7:51–56.

Budinger, T.F., 1967. Cobb Seamount. *Deep-Sea Res. Part A,* 14:191–201.

Buigies, D., 1985. Principal facies and their distribution at Mururoa Atoll. *Proc. 5th Int. Coral Reef Congr.,* 3:249–255.

Calmant, S., and Cazenave, A., 1986. The effective elastic lithosphere under the Cook-Austral and Society islands. *Earth Planet. Sci. Lett.,* 77:187–202.

————, 1987. Anomalous elastic thickness of the oceanic lithosphere in the south-central Pacific. *Nature,* 328:236–238.

Cheminee, L.L., Hekinian, R., Talandier, J., Albarede, F., Devey, C.W., Francheteau, J., and Lancelot, Y., 1989. Geology of an active hotspot: Tehatia-Mehetia region in the south-central Pacific. *Mar. Geophys. Res.,* 11:27–50.

Clague, D.A., and Dalrymple, G.B., 1989. Tectonics, geochronology, and origin of the Hawaiian-Emporer volcanic chain. *In* Winterer, E.L., Hussong, D.M., and Decker, R.W. (Eds.), *The Eastern Pacific Ocean and Hawaii.* Geol. Soc. Am., Geol. of North America Ser., N:188–217.

Cole, W.S., 1954. Larger foraminifera and smaller diagnostic foraminifera from Bikini drill holes. *Geol. Surv. Prof. Pap. U.S.,* 260-O:569–608.

Crough, S.T., 1983a. Hotspot swells. *Annu. Rev. Earth Planet. Sci.,* 11:165–193.

————, 1983b. The correction for sediment loading on the seafloor. *J. Geophys. Res.,* 88:6449–6454.

Davies, P.J., Marshall, J.F., and Hopley, D., 1985. Relationships between reef growth and sea level in the Great Barrier Reef. *Proc. 5th Int. Coral Reef Symp.,* 3:95–103.

Davis, A.S., Pringle, M.S., Pickthorn, L.B.G., Clague, D.A., and Schwab, W.C., 1989. Petrology and age of alkalic lava from the Ratak Chain of the Marshall Islands. *J. Geophys. Res.,* 94:5757–5774.

Detrick, R.S., and Crough, S.T., 1978. Island subsidence, hot spots, and lithospheric thinning. *J. Geophys. Res.,* 83:1236–1244.

Duncan, R.A., and McDougall, I., 1974. Migration of volcanism with time in the Marquesas Islands, French Polynesia. *Earth Planet. Sci. Lett.,* 21:414–420.

————, 1976. Linear volcanism in French Polynesia. *J. Volcanol. Geotherm. Res.,* 1:197–227.

Duncan, R.A., McDougall, I., Carter, R.M., and Coombs, D.S., 1974. Pitcairn Island—another Pacific hotspot? *Nature,* 251:679–682.

Emery, K.O., Tracey, J.I., Jr., and Ladd, H.S., 1954. *Geology of Bikini and Nearby Atolls.* Geol. Surv. Prof. Pap. U.S., 260-A.

Filmer, P., McNutt, M., and Wolfe, C., 1993. Elastic thickness of the lithosphere in the Society and Marquesas islands: no evidence for elastic plate thinning over the South Pacific Superswell. *Eos,* 74:284.

Fiske, R.S., and Jackson, E.D., 1972. Orientation and growth of Hawaiian volcanic rifts: the effect of regional structure and gravitational stresses. *Proc. R. Soc. London A,* 329:299–326.

Grigg, R.W., 1982. Darwin Point: a threshold for atoll formation. *Coral Reefs,* 1:29–34.

Grigg, R.W., and Epp, D., 1989. Critical depth for the survival of coral islands: effects on the Hawaiian Archipelago. *Science,* 243:638–641.

Hamilton, E.L., and Rex, R.W., 1959. Lower Eocene phosphatized *Globigerina* ooze from Sylvania Guyot. *Geol. Surv. Prof. Pap. U.S.,* 260-W:785–797.

Harland, W.B., Armstrong, R.L., Cox, A.V., Craig, L.E., Smith, A.G., and Smith, D.G., 1990. *A Geologic Time Scale 1989:* Cambridge (Cambridge Univ. Press).

Hart, S.R., 1984. A large-scale isotope anomaly in the Southern Hemisphere mantle. *Nature,* 309:753–757.

Hein, J.R., Kang, J.K., et al., 1990. Geological, geochemical, geophysical, and oceanographic data and interpretations of seamounts and C-rich ferromanganese crusts from the Marshall Islands, KORDI-USGS R.V. *Faranella* cruise F10-89-CP. *Open-File Rep.—U.S. Geol. Surv.,* 90-407.

Hopley, D., 1982. *The Geomorphology of the Great Barrier Reef: Quaternary Development of Coral Reefs:* New York (Wiley).

Jarrard, R.D., and Turner, D.L., 1979. Comments on "Lithospheric flexure and uplifted atolls" by M. McNutt and H.W. Menard. *J. Geophys. Res.,* 84:5691–5697.

Johnson, H.P., and Helferty, M., 1990. The geological interpretation of side-scan sonar. *Rev. Geophys.,* 28:357–380.

Lambeck, K., 1981. Flexure of the ocean lithosphere from island uplift, bathymetry and geoid height observations: the Society Islands. *Geophys. J. R. Astron. Soc.,* 67:91–114.

Larson, R.L., 1992. Geological consequences of superplumes. *Geology,* 19:963–966.

Larson, R.L., Schlanger, S.O., et al., 1981. *Init. Repts. DSDP,* 61: Washington (U.S. Govt. Printing Office).

Lincoln, J.M., 1990. Regional tectonic history and Cenozoic sea levels deduced from drowned carbonate banks and atoll stratigraphy in the Marshall Islands, west central Pacific Ocean [Ph.D. dissert.]. Northwestern Univ., Evanston, IL.

Lincoln, J.M., Pringle, M.S., and Premoli-Silva, I., 1993. Early and Late Cretaceous volcanism and reef-building in the Marshall Islands. *In* Pringle, M.S., Sager, W.W., Sliter, W.V., and Stein, S. (Eds.), *The Mesozoic Pacific: Geology, Tectonics, and Volcanism.* Geophys. Monogr., Am. Geophys. Union, 77:279–305.

Lonsdale, P., Normark, W.R., and Newman, W.A., 1972. Sedimentation and erosion on Horizon Guyot. *Geol. Soc. Am. Bull.,* 83:289–315.

McNutt, M.K., and Fischer, K.M., 1987. The South Pacific superswell. *In* Keating, B.H., Fryer, P., Batiza, R., and Boehlert, G.W. (Eds.), *Seamounts, Islands, and Atolls.* Geophys. Monogr., Am. Geophys. Union, 43:25–34.

McNutt, M.K., and Judge, A.V., 1990. The Superswell and mantle dynamics beneath the South Pacific. *Science,* 248:969–975.

McNutt, M.K., and Menard, H.W., 1978. Lithospheric flexure and uplifted atolls. *J. Geophys. Res.,* 83:1206–1212.

McNutt, M.K., Winterer, E.L., Sager, W.W., Natland, J.H., and Ito, G., 1990. The Darwin Rise: a Cretaceous superswell? *Geophys. Res. Lett.,* 17:1101–1104.

Menard, H.W., 1964. *Marine Geology of the Pacific:* New York (McGraw-Hill).

————, 1983. Insular erosion, isostacy, and subsidence. *Science,* 220:913–918.

Menke, W., and Abbott, D., 1990. *Geophysical Theory:* New York (Columbia Univ. Press).

Moberly, R., and Jenkyns, H.C., 1981. Cretaceous volcanogenic sediments of the Nauru Basin, Deep Sea Drilling Project Leg 61. *In* Larson, R.L., Schlanger, S.O., et al., *Init. Repts. DSDP,* 61: Washington (U.S. Govt. Printing Office), 533–548.

Moberly, R., Schlanger, S.O., et al., 1986. *Init. Repts. DSDP,* 89: Washington (U.S. Govt. Printing Office).

Moore, J.G., and Clague, D.A., 1992. Volcano growth and evolution of the island of Hawaii. *Geol. Soc. Am. Bull.,* 104:1471–1484.

Moore, J.G., Clague, D.A., Holcomb, R.T., Lipman, P.W., Normark, W.R., and Torresan, M.E., 1989. Prodigious submarine landslides on the Hawaiian Ridge. *J. Geophys. Res.,* 94:17465–17484.

Nakanishi, M., Gee, J., and ODP Leg 144 Shipboard Scientific Party, 1992a. Paleolatitude of guyots in the northwestern Pacific Ocean: preliminary results of ODP Leg 144. *Eos,* 73:586–587.

Nakanishi, M., Tamaki, K., and Kobayashi, K., 1992b. A new Mesozoic isochron chart of the northwestern Pacific Ocean: paleomagnetic and tectonic implications. *Geophys. Res. Lett.,* 19:693–696.

Nishimura, C.E., and Forsyth, D.W., 1985. Anomalous Love-wave phase velocities in the Pacific: sequential pure-path and spherical harmonic inversion. *Geophys. J. R. Astron. Soc.,* 81:389–407.

Parsons, B., and Sclater, J.G., 1977. An analysis of the variation of ocean floor bathymetry and heat flow with age. *J. Geophys. Res.,* 82:803–829.

Pratt, R.M., 1963. Great Meteor Seamount. *Deep-Sea Res. Part A,* 10:17–25.

Premoli Silva, I., Haggerty, J., Rack, F., et al., 1993. *Proc. ODP, Init. Repts.,* 144: College Station, TX (Ocean Drilling Program).

Premoli Silva, I., and Sliter, W.V., 1981. Cretaceous planktonic foraminifers from the Nauru Basin, Leg 61, Site 462, western equatorial Pacific. *In* Larson, R.L., Schlanger, S.O., et al., *Init. Repts. DSDP,* 61: Washington (U.S. Govt. Printing Office), 423–438.

Pringle, M.S., 1992. Geochronology and petrology of the Musicians Seamounts, and the search for hot spot volcanism in the Cretaceous Pacific [Ph.D. dissert.]. Univ. of Hawaii, Honolulu.

Pringle, M.S., and Staudigel, H., 1992. Age and distribution of Cretaceous Pacific seamount volcanism. *Eos,* 73:586.

Raitt, R.W., 1954. Seismic refraction studies of Bikini and Kwajalein atolls. *Geol. Surv. Prof. Pap. U.S.,* 260-K:507–527.

Schlager, W., 1981. The paradox of drowned reefs and carbonate platforms. *Geol. Soc. Am. Bull.,* 92:197–211.

Schlanger, S.O., 1963. Subsurface geology of Eniwetak Atoll. *Geol. Surv. Prof. Pap. U.S.,* 260-BB:991–1066.

Schlanger, S.O., Campbell, J.F., and Jackson, M.W., 1987. Post-Eocene subsidence of the Marshall Islands recorded by drowned atolls on Harrie and Sylvania guyots. *In* Keating, B.H., Fryer, P., Batiza, R., and Boehlert, G.W. (Eds.), *Seamounts, Islands, and Atolls.* Geophys. Monogr., Am. Geophys. Union, 43:165–174.

Schlanger, S.O., and Premoli Silva, I., 1981. Tectonic, volcanic, and paleogeographic implications of redeposited reef faunas of Late Cretaceous and Tertiary age from the Nauru Basin and the Line Islands. *In* Larson, R.L., Schlanger, S.O., et al., *Init. Repts. DSDP,* 61: Washington (U.S. Govt. Printing Office), 817–827.

Shor, A., 1990. SeaMARC II seafloor mapping system: seven years of Pacific research. *Proc. Pac. Rim Congr. 90,* 3:49–59.

Smith, W.H.F., 1990. Geophysics of Ratak Guyot (Marshall Islands): implications for the history of the South Pacific Isotopic and Thermal Anomaly. *Eos,* 71:1667.

Smith, W.H.F., Staudigel, H., Watts, A.B., and Pringle, M.S., 1989. The Magellan Seamounts: Early Cretaceous record of the south Pacific isotopic and thermal anomaly. *J. Geophys. Res.,* 94:10501–10523.

Stoffers, P., Botz, R., Cheminee, R.-L., Devey, C.W., Froger, V., Glasby, G.P., Hartmann, M., Hekinian, R., Kogler, F., Laschek, D., Larque, P., Michaelis,W., Muhe, R.K., Puteanus, D., and Richnow, H.H., 1989. Geology of Macdonald Seamount region, Austral Islands: recent hotspot volcanism in the South Pacific. *Mar. Geophys. Res.,* 11:101–112.

Takigami, Y., Amari, S., Ozima, M., and Moberly, R., 1986. $^{40}Ar/^{39}Ar$ geochronological studies of basalts from Hole 462A, Nauru Basin, Deep Sea Drilling Project Leg 89. *In* Moberly, R., Schlanger, S.O., et al., *Init. Repts. DSDP,* 89: Washington (U.S. Govt. Printing Office), 519–522.

Turner, D.L., and Jarrard, R.D., 1982. K-Ar dating of the Cook-Austral island chain: a test of the hotspot hypothesis. *J. Volcanol. Geotherm. Res.,* 12:187–220.

Vail, P.R., Mitchum, R.M., Jr., Todd, R.G., Widmier, J.M., Thompson, S., III, Sangree, J.B., Bubb, J.N., and Hatlelid, W.G., 1977. Seismic stratigraphy and global changes in sea level. *In* Payton, C.E. (Ed.), *Seismic Stratigraphy—Applications to Hydrocarbon Exploration.* AAPG Mem., 26:49–221.

Vogt, P.R., and Smoot, N.C., 1984. The Geisha Guyots: multibeam bathymetry and morphometric interpretation. *J. Geophys. Res.,* 89:11085–11107.

Walker, D.A., and McCreery, C.S., 1988. Deep-ocean seismology: seismicity of the northwestern Pacific Basin interior. *Eos,* 69:737.

Watts, A.B., and ten Brink, U.S., 1989. Crustal structure, flexure, and subsidence history of the Hawaiian Islands. *J. Geophys. Res,* 94:10473–10500.

Weins, H.J., 1962. *Atoll Environment and Ecology:* New Haven (Yale Univ. Press).

Wessel, P., and Smith, W.H.F., 1991. Free software helps map and display data. *Eos,* 72:441–446.

Wilson, J.L., 1975. *Carbonate Facies in Geologic History:* Berlin (Springer-Verlag).

Date of initial receipt: 7 February 1994
Date of acceptance: 15 September 1994
Ms 144SR-019

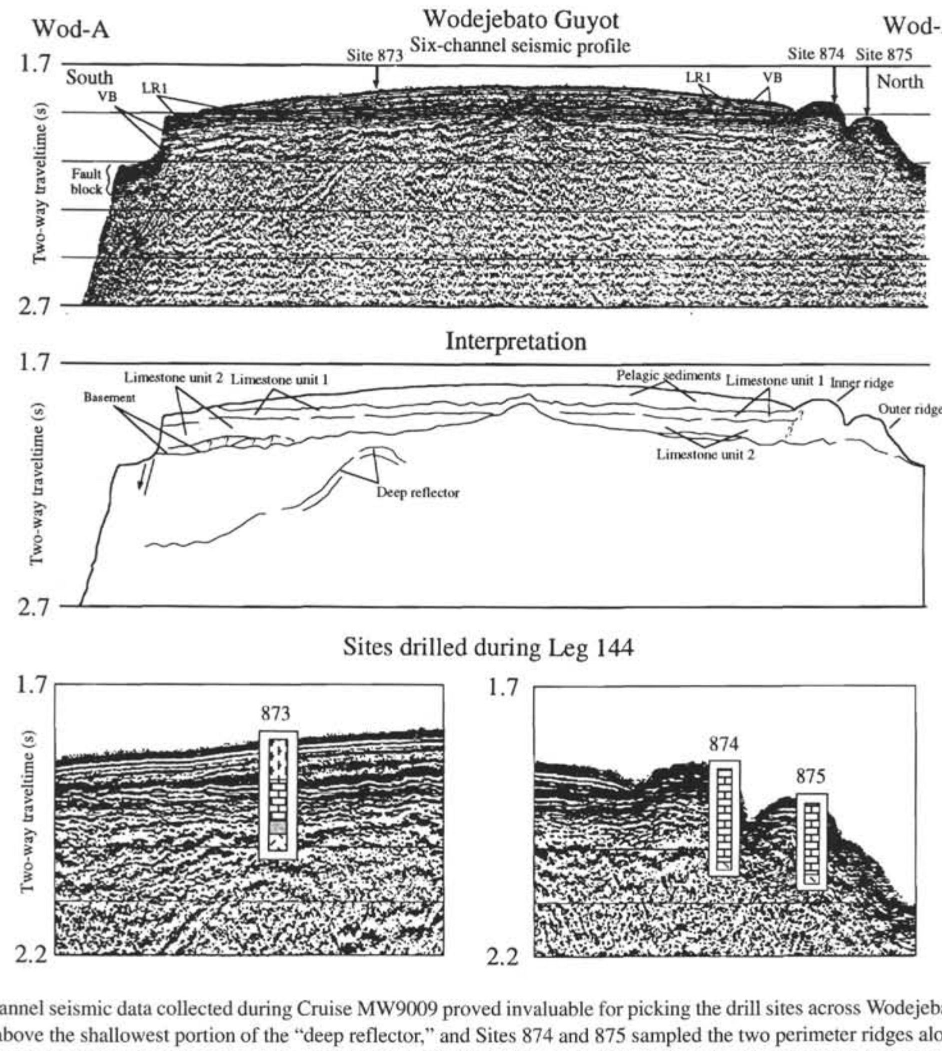

Figure 21. The six-channel seismic data collected during Cruise MW9009 proved invaluable for picking the drill sites across Wodejebato Guyot. Site 873 sampled the lagoon sediment above the shallowest portion of the "deep reflector," and Sites 874 and 875 sampled the two perimeter ridges along the northeast edge of the summit plateau. Two primary sediment units compose the shallow-water platform carbonates (denoted by the reflectors LR1 and LR2). Reflectors within the lower unit truncate against the central basement high. The deep reflector noted on Lo-En Guyot also appears as a sub-basement reflector on this guyot. Lithologic symbols identical to those shown in Figure 20. Profile location is shown in Figure 11.

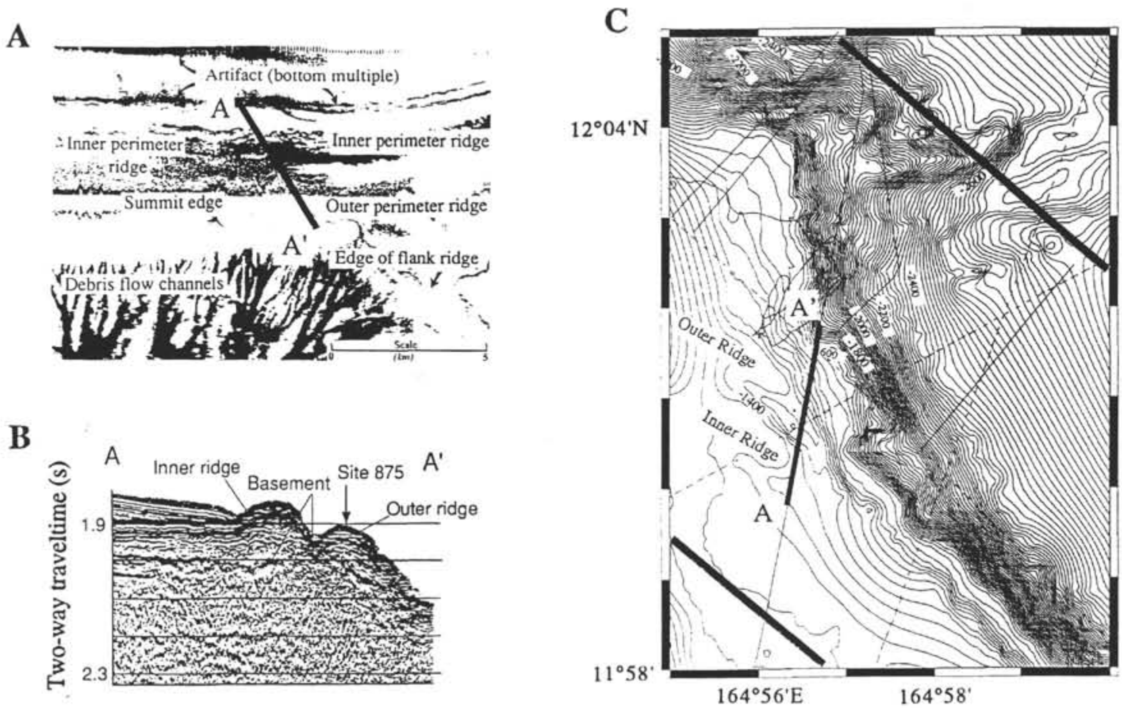

Figure 22. Sidescan image across the northeast flank ridge of Wodejebato Guyot (**A**) shows the perimeter ridges drilled during Leg 144. Similar to the case on the north flank ridge, the outer perimeter ridge widens across the shelf formed by the northeast flank ridge. The six-channel seismic profile (**B**) collected during Cruise MW9009 reveals the internal structure of the perimeter ridges in more detail than the single-channel profile presented in Figure 22. SeaBeam bathymetry (**C**) collected over this same area during the *Thomas Washington* Cruise TUNE06 (H. Staudigel, unpubl. data, 1989) helps define the changes in perimeter ridge topography toward the edge of the shelf. Note the channel separating the inner and outer perimeter ridges, and the loss of relief across the outer ridge toward the edge of the shelf. Sidescan image location is shown in Figure 11. The contour interval is 20 m.

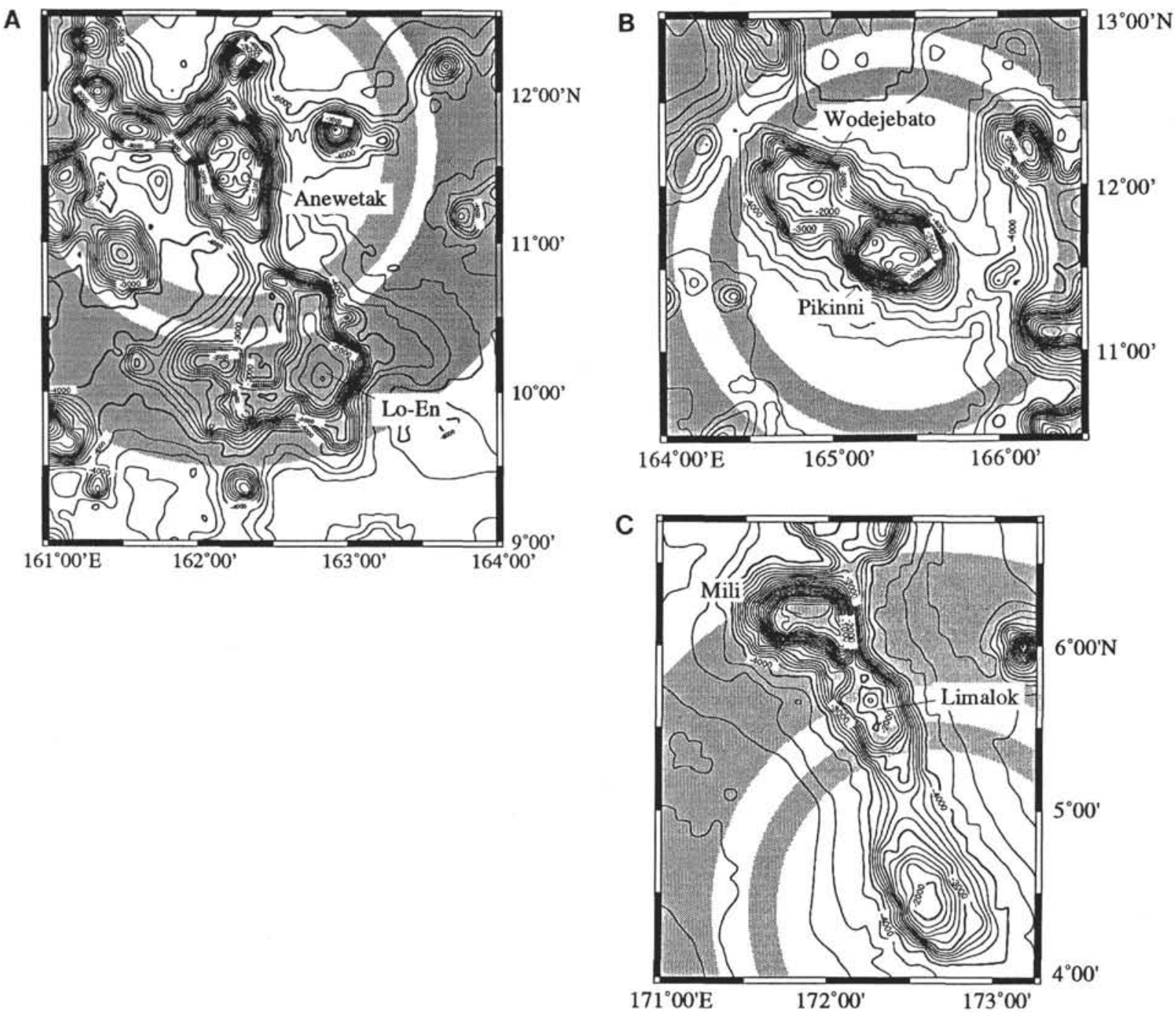

Figure 23. Flexure modeling for the atoll and guyot pairs of Anewetak and Lo-En, Pikinni and Wodejebato, and Mili and Limalok. Each map shows two gray bands. The inner band marks the 300-m-downward deflection contour for a plate varying in thickness from 10 (inner edge) to 20 km (outer edge). The outer band marks the 0-m deflection contour for a similarly varying plate. For Anewetak and Lo-En (**A**), the load added to the plate was the volcanic edifice of Anewetak. Lo-En lies squarely in the region of 0 deflection from this load. For Pikinni and Wodejebato (**B**), the load added to the plate was the volcanic edifice beneath Pikinni Atoll. Wodejebato lies slightly within the region of 300-m-downward deflection, yet neither the volcanic platform nor the carbonate platform appear tilted toward Wodejebato. The lack of tilting suggests that both edifices were erupted at approximately the same time. For Mili and Limalok (**C**), the load added to the plate was the volcanic edifice south of Limalok. Limalok lies slightly inside the region of 0-m deflection, which may explain the pattern of prograding basement reflectors along the south flank of this guyot.